Author's response

Responses to Anonymous Referee #1

For clarity we repeat the reviewer comments in normal font, followed by our responses in blue italic font.

In their paper "Recent satellite-based trends of tropospheric nitrogen dioxide over large urban agglomerations worldwide", Schneider et al. report on NO2 trends derived from SCIAMACHY satellite observations over megacities and large agglomerations. They give results for 66 regions, provide a brief statistical analysis of the distribution of trends, investigate the average behaviour of NO2 in all agglomerations combined and also separated by geographical region, briefly investigate the impact of spatial resolution on the derived trends and finally analyse the link between population growth and NO2 change.

NO2 is an interesting proxy for air pollution and one of the atmospheric composition parameters which can be observed well from space. Previous publications have highlighted large changes in tropospheric NO2 amounts over the last 15 years but have not covered as many individual regions as this paper. As I'm sure that this overview (mainly Table 3 of the paper) will be of interest to many readers, and because the study is well written and sound, I can recommend it for publication in ACP after consideration of the points made below.

We thank the reviewer *for the overall positive assessment.*

General Comments:

The amount of new material in this manuscript and the progress beyond the state of art (and beyond the last paper of the same authors) is rather limited, and one would hope that a follow-up publication on a topic so thoroughly investigated in literature as NO2 trends from satellite would contain more original data and conclusions.

The manuscript is intended as a follow-up to the Schneider et al. 2012 JGR paper allowing us to go into more detail about specific trends over a very large number of urban agglomerations worldwide. To our knowledge, our study provides what is currently the most comprehensive analysis of NO2 trends over urban agglomerations worldwide, significantly expanding the number of study sites from that of previous studies (e.g. Schneider et al. 2012 or Hilboll et al., 2013). As such, one of the main outputs of the study is the overview of trends for a large number of urban sites computed from a reliable and homogeneous data source (as mentioned by the reviewer above). In addition to the, at least to our knowledge, most comprehensive global overview of NO2 trends over urban areas to date, the paper further provides the first-ever comparison of NO2 trends with changes in population density.

Nonetheless, following the reviewer's advice we have now significantly expanded several sections of the manuscript to go into more detail on several relevant issues. We have substantially improved the background section by providing a much broader overview of *the relevant literature. We also added an additional figure showing an example of the trend fitting results and discuss this additional figure in detail, as well as the implications of errors in the model fit on the trend assessment. Furthermore, we significantly expanded the section on the relationship between population growth and NO2 trends and in the revised manuscript now provide additional material discussing potential reasons for the observed clustering effects.*

The link to the MACC-II project and thus the Special Issue is limited to the source of funding. The paper does not discuss in any way the connection to the COPERNICUS system, presumably because there is none, and I think it should not be part of this Special Issue.

The study was carried out through partial funding provided by the MACC-II project. More specifically, the OBS subproject, as part of which we performed this work, has the goal of evaluating satellite data related to Copernicus. Future Copernicus satellites such as Sentinel-5p, Sentinel-5, and Sentinel-4 will continue the NO_2 record provided by SCIAMACHY and other satellite instruments. Thus, the study of NO2 trends from predecessor satellite instruments is very relevant for users of NO2 data from the future Copernicus satellites, both for extending the NO2 trends and for assessing the quality of NO2 data from these future satellites. Furthermore, there is a strong link between trends in satellite-based NO2 columns and changes in NOx emissions, which in turn have an important effect on the quality of the results provided by the Copernicus Atmospheric Monitoring Service (CAMS). For these reasons, we think it is appropriate for this paper to be included in the MACC-II special issue.

In order to clarify these points and to highlight the relevance of our study for Copernicus we have revised this section and further added additional material in the introduction.

Throughout the paper and the figure captions, the authors use the term "concentrations" where they really mean "tropospheric columns". This has to be corrected.

We note that many other studies have used the term "concentrations" in lieu of "columns" when talking about satellite-derived tropospheric NO2 data; examples include van der A et al. (2008), Castellanos and Boersma (2012), and Curier et al. (2014). However, we do agree with the referee that "tropospheric column" is the more technically correct term and we modified the manuscript accordingly.

Figure 1 is nice but has two problems that the authors should fix:

1. There is a clear stripy pattern visible which is not present in other SCIAMACHY NO2 figures published in the literature.

2. There is clear indication for a shipping signal between Central America and Europe. To my knowledge, this is an artefact which should not be present or at least should be mentioned in the figure caption.

1) The origin of the stripy pattern is not entirely clear, but likely related to an east-west difference across the swath in combination with the repeating orbit cycle. Earlier studies (e.g., van der A et al. 2008) have noticed this artefact; however, this effect was not as *obvious in, e.g., van der A et al., due to a different color scale used in their figure. Since the stripy pattern occurs only over the ocean and since the tropospheric columns there are extremely low (< 0.3 * 10^{15} molec cm^2), they occur in regions where NO2 measurements are mostly below the detection limit of the SCIAMACHY instrument. Because of this, we think it is justified to modify the color scale slightly to mask out the stripy pattern. Please note that because none of our urban agglomeration study sites exhibit such low long-term average values or are located anywhere near the stripes which are visible only over the oceans, the analysis carried out in this paper is unaffected by the striping issue.*

*2) This linear feature is a known artefact and not a real shipping signal. It originates from the TM4 Chemical Transport Model used in the TEMIS retrieval process. While it is an artefact in the dataset, it should be noted that the signal is extremely small (approximately 0.32 * 10^{15} molec cm^2 versus 0.24 * 10^{15} molec cm^2 in the surrounding background over the Atlantic Ocean, i.e., an enhancement of roughly 0.06 * 10^{15} molec cm^2). While this issue is known, it has hitherto not been visible in similar figures because of the different color scales used. Again, please note that none of the urban agglomerations studied here are affected by this artefact as they are not located anywhere in their vicinity.*

We very slightly modified the lower part of the color scale of Figure 1 to bring it more in line with what previous studies have shown and mask the striping artefacts which are irrelevant for this study. We further included a comment in the Figure caption noting that the faint linear feature in the North Atlantic is not a real signal but an artefact originating from the particular model-based retrieval methodology used by TEMIS. The updated Figure 1 is shown below.

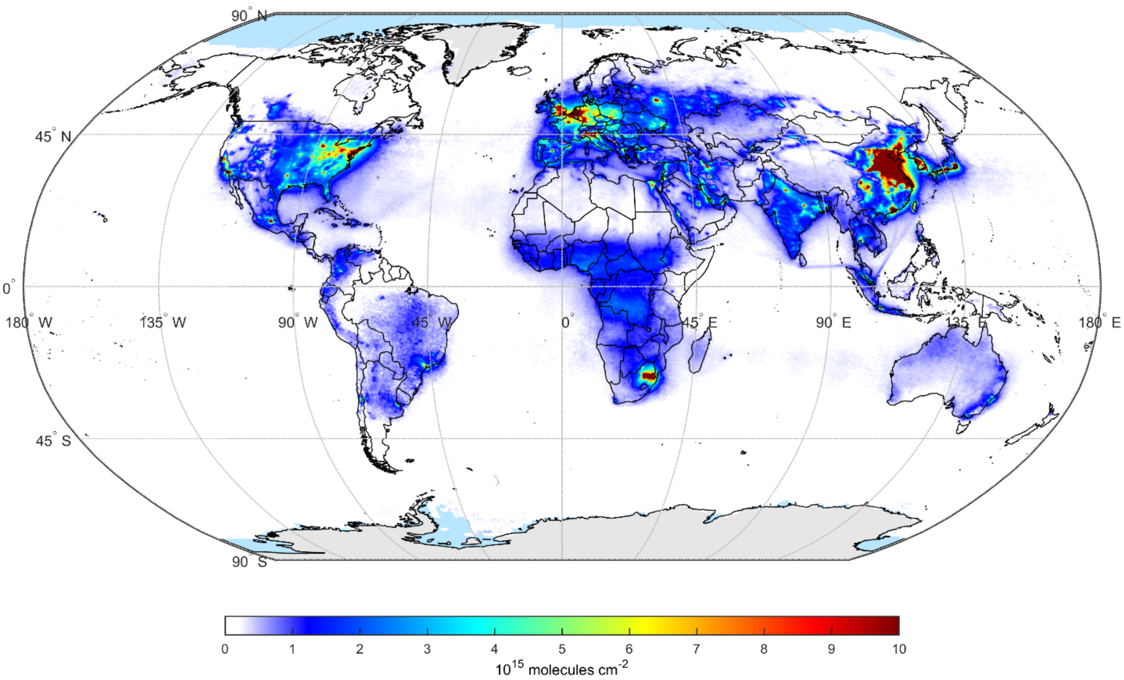

Figure 1 updated based on the reviewer comments. The striping pattern, which was only visible due to the very detailed color scale that we used (in particular for the lower part of the scale), is now gone. The faint linear feature in the North Atlantic is now mentioned in the updated Figure caption.

The 2008 drop in Figure 4 is obvious and tempting to link to the economic downturn. However, if we believe this, what is then the explanation for the rapid increase in 2004?

We were at first slightly puzzled about what could be the cause for this increase in 2004. It turns out this effect might also be related to changes in economic activity, which we were able to show by comparing the data to an index of economic health (see updated Figure 5). This leading economic index shows an increase throughout 2003 that precedes the NO2 concentration increase. Similarly, this economic index shows a decrease in mid-2007 preceding the big drop in NOx emissions associated with the global economic crisis.

We took this opportunity to revisit the underlying analysis and improve the Figure (former Figure 4, Figure 5 in the revised manuscript) in several aspects. Firstly, we included a time series of the fitted model together with the global average time series of NO2 VCDs. Secondly, we included an additional panel showing the residuals of the model fit. Thirdly, we included an additional panel showing the temporal behavior of an economic index (the ECRI Weekly leading index). We further added gray boxes identifying to the reader the two periods of interest (2003-2004 and 2007-2008).

We also included an additional description of the Figure and a discussion and interpretation of the results:

"Figure 4c also indicates an increase from late 2003 through early 2004. The reason for this behavior is not as obvious. To better understand this feature, Figure 4d shows a monthly-averaged time series of the Economic Cycle Research Institute (ECRI) leading weekly economic index (https://www.businesscycle.com/ecri-reports-indexes/all-indexes). While this index is primarily intended as an indicator of the economic outlook for the United States (higher values indicate a more positive outlook), we use it here as a proxy for the global economic situation. Both the increase in 2003/2004 and the rapid drop in 2008 are clearly seen in both datasets, suggesting a link between the NO2 levels over large urban agglomerations and the economic situation. It should be noted that other features such as the small temporary decrease in NO2 levels in 2006 (Figure 4c), or the moderate rise of the NO2 levels in 2010, are not reflected as clearly by the economic index. However, the latter could be interpreted as a slightly delayed response, keeping in mind that the NO2 levels shown in Figure 4c are global averages whereas the economic index shown in Figure 4d is for the United States. Overall, these results indicate that the global average NO2 levels over major urban agglomerations reflect large-scale changes in the global economic situation that happen over a relatively short timeframe."

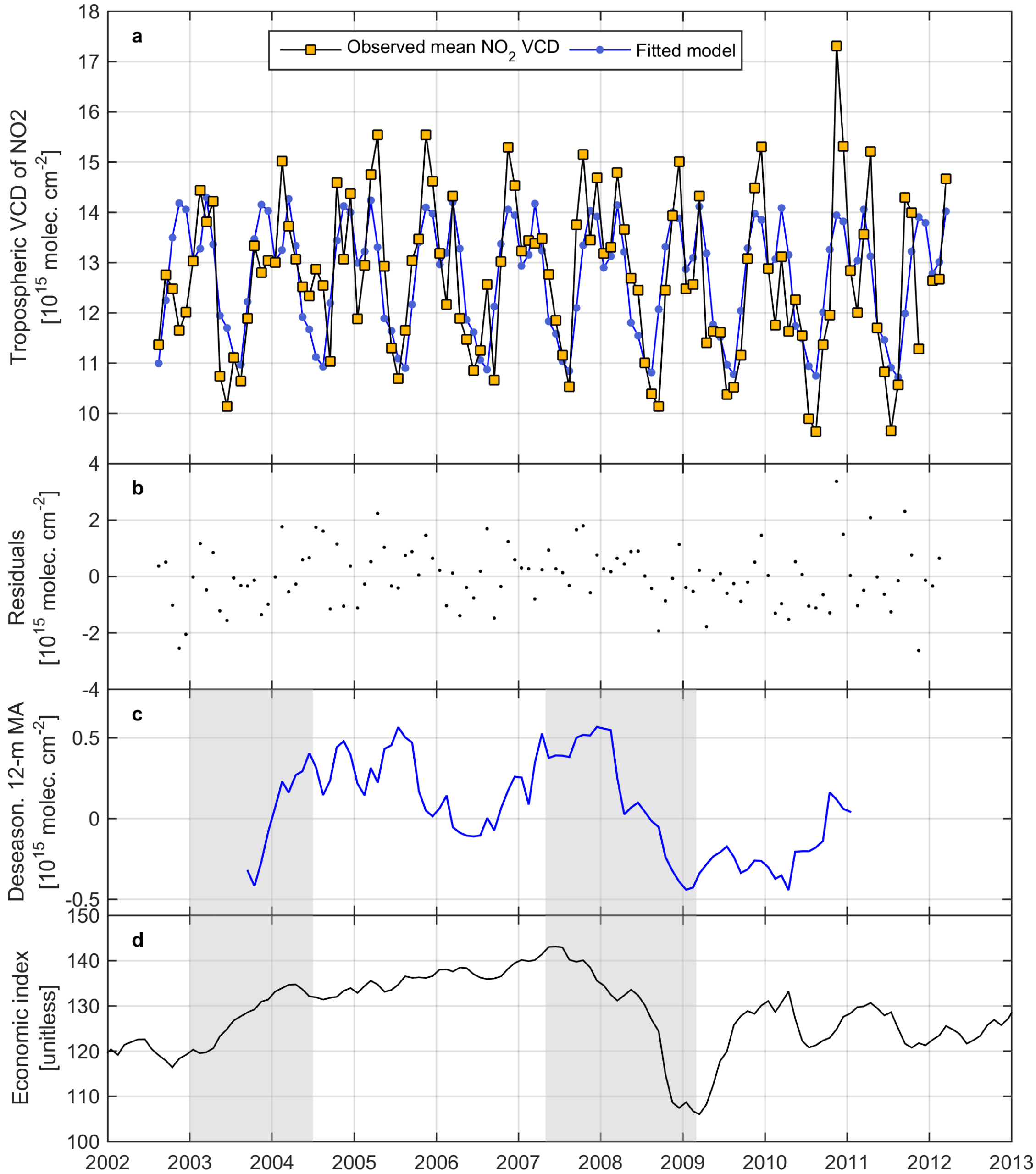

IMPROVED AND EXPANDED FIGURE 4. Average time series of SCIAMACHY-derived tropospheric NO2 column computed over all study sites including a fitted trend model (a), the model residuals (b), the 12-month moving average of the deseasonalized time series (c), and the ECRI Weekly Economic Index. Gray boxes in the two lowermost panels mark periods where the overall NO2 levels in the studied urban agglomerations are indicative of overall economic activity.

As this study uses values from individual grid cells, it would be good to add information how exactly the SCIAMACHY observations were mapped into the grid.

We included a brief description of the gridding process in the revised manuscript (Section 3.1).

Specific Comments:

p24313,l2: “strongly increased emissions” – relative to what?

Revised to “very high emissions”

p24314,l17: ERS-1 => ERS-2

Many thanks for this correction. This has been fixed.

p24315,l2: using method => using a method

Fixed.

p24316,l14: in spite of its name, SCIAMACHY does not have imaging spectrometers so I’d suggest to drop “imaging” here

Thanks for this advice. We dropped the term “imaging” in the revised manuscript.

24318,l11: statistic model => statistical model

Fixed.

p24318,l21: it might be worthwhile to mention here that the seasonality is assumed to be constant over time

Agreed. We added a clarifying statement on this.

p24319,l17: Adding 1015 here doesn’t make sense as the units just have to be the same as for the mean columns.

Agreed. This has been taken out and replaced by “given in units of molecules cm^{-2} year^{-1}”

p24319,l20: Is VCDtrop deseasonalised?

No, it is the long-term average of the original column values. We added a statement on this in the revised manuscript.

p24321,l12: value => values

This has been corrected.

p24321,l17: “most rapidly increasing trend” – I guess not the trend is increasing but the columns

Correct. We replaced this phrase with “is the site with the largest relative trend” in order to make this less ambiguous.

p24325,l24 “politically motivated emission reductions” => suggest to rephrase this to something like “emission reductions linked to changes in legislation”

We changed this phrase based on the reviewer’s suggestion.

p24326,l20: Something is wrong with this list – 45 sites have statistically significant trends, of those 34 increasing, 24 of which are statistically significant?

This statement was unclear – thank you for bringing this to our attention. We changed this to

“Overall, 44 of the 66 study sites showed statistically significant trends (either positive or

negative) at the 95% level. In total, 34 sites exhibited increasing levels of tropospheric NO2 throughout the study period, 24 of which were found to be statistically significant. In addition,
32 sites showed decreasing levels of tropospheric NO2 during the study period, of which 20 sites did so at statistically significant magnitudes."

p24327,l6: characteristics patterns => characteristic patterns

Fixed.

Table 2, what is N?

We understand this refers to Table 3, not Table 2 as the latter does not contain an N. As for Table 3, N was not defined in the caption. We therefore added a statement about N in the caption of Table 3.

Figure 2: studies urban => studied urban

Corrected.

Figure 3: trend over => trends over

Corrected.

Responses to Anonymous Referee #2

For clarity we repeat the reviewer comments in normal font, followed by our responses in *blue italic font*.

The manuscript presents trends in tropospheric NO2 over large urban agglomerations. The authors used a fit of SCIAMACHY NO2 columns to a statistical model with a linear trend and seasonal component to derive the trend. The main innovations of the work are that the scope both in number and location of the urban agglomerations has been expanded, and a comparison of the NO2 trend was made to population growth estimates. The manuscript is well written and concise, and presents results that would be useful to the atmospheric science community. Therefore it deserves to be published.

We thank the reviewer for the overall positive assessment.

However, the manuscript would benefit from an expanded and more detailed discussion of the current literature on global and regional NO2 trends, and some explanation for the results regarding the relationship between NO2 trend and population growth. In Section 3.3, I think it is important to show examples of the fit to the NO2 time series, and to include some discussion on the quality of the fit and how this could effect the trend calculations.

We significantly expanded the background section in order to discuss more of the relevant current literature, including all papers specifically recommended by the reviewer, and several more (see the more detailed comments below). Based on the reviewer's recommendation we further expanded the discussion of the results between NO2 trends and population growth taking into account recent published studies such as Lamsal et al. 2013. In Section 3.3 we followed the advice of the reviewer and included an additional Figure (Figure 2 in the revised paper) giving an example of the fit to the NO2 time series, as shown for the example of Baghdad, Iraq. We further included a comprehensive discussion of this Figure and added material discussing the quality of the fit and its potential effect on trend calculations.

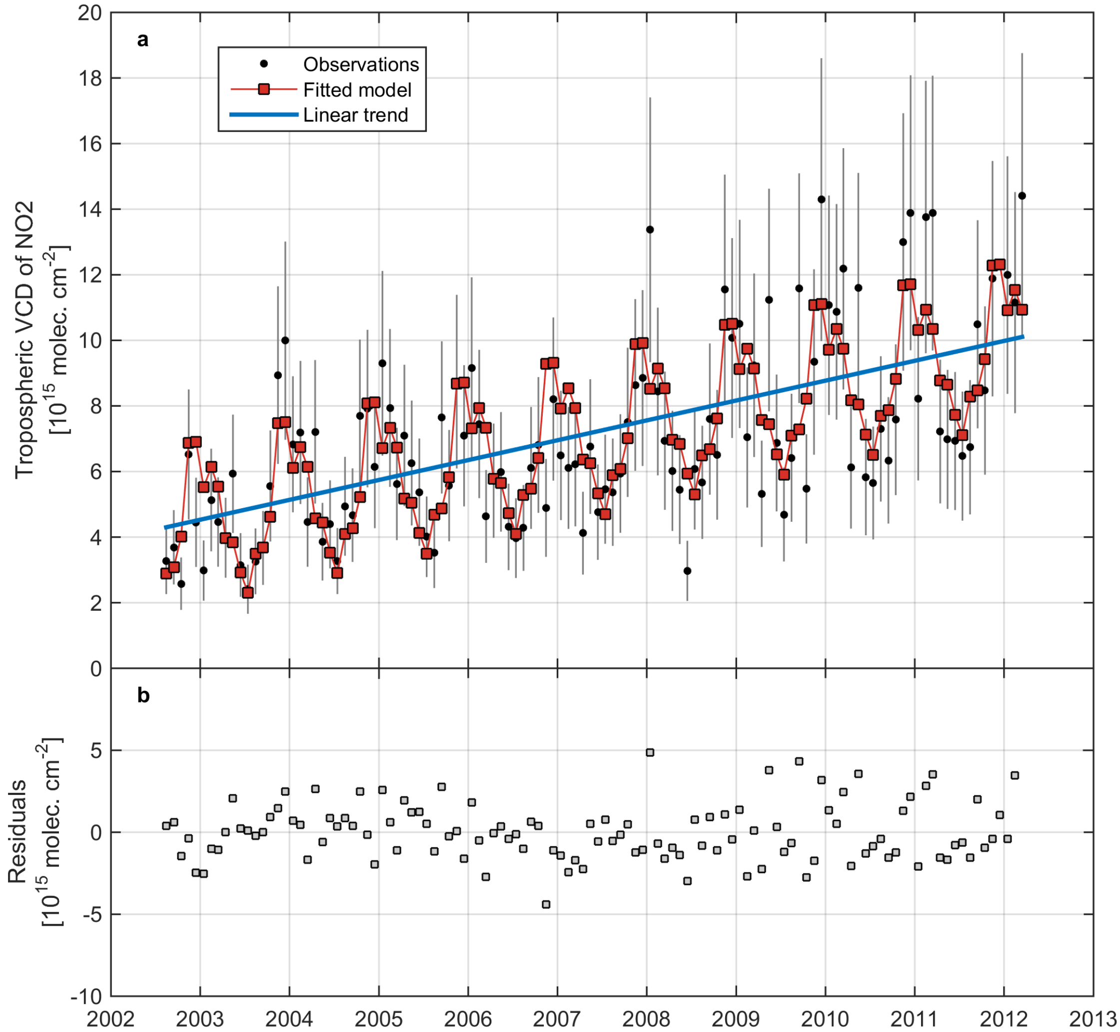

Figure 2: Additional Figure added in Section 3.3 to show an example of the model fit to the NO2 time series

Below are some specific comments:

Page 24313 Line 16-25: The writer states that in the context of the MACC chemical weather forecasting framework the purpose of the work is to test whether SCIAMACHY observations could be useful for estimating trends. It's not clear how chemical weather forecasting and NO2 trends from SCIAMACHY are related. SCIAMACHY stopped reporting data in 2012, therefore no new data could be available for forecasting purposes. Some explanation of this should be made here.

The reviewer is correct that SCIAMACHY is no longer operational. However, we see this study as contributing toward preparation for the upcoming Copernicus satellite instruments related to atmospheric composition. Future Copernicus satellites such as Sentinel-5p, Sentinel-5, and Sentinel-4 will carry on the existing NO2 record provided by SCIAMACHY, OMI, and GOME-2. The methodology and results obtained for a predecessor instrument will be applicable and relevant for the Copernicus-funded successor instruments. Furthermore, there is a strong link between trends in satellite-based NO2 columns and changes in NOx emissions, which in turn have an important effect on the *quality of the results provided by the Copernicus Atmospheric Monitoring Service (CAMS). We also address this point in the response to Reviewer 1.*

To clarify these points, and to highlight the relevance of our study for Copernicus more clearly, we have revised this section and added additional material in the introduction.

Page 24314 Line 15: In this section, references to the following recent papers on satellite-based NO2 trends are missing: Zhou et al., Atmospheric Environment (2012). Castellanos and Boersma, Scientific Reports (2012). Curier et al., Remote Sensing of the Environment (2014). In fact, it may be useful to include a table or a simple figure illustrating the findings of past studies, of which at this point there are many.

Thank you for this comment. Not including these references was an oversight and we now add them in this section and include a short summary for each of them. We took this opportunity to significantly expand the background section and we now cite and briefly summarize/discuss many other additional relevant publications, including Meena et al. (2012), Hayn et al. (2009), Sitnov (2011), Guerreiro (2014), World Health Organization (2013), Martin (2008), Duncan et al. (2014), Ionov (2010), Liu and Zhu (2013), and Burrows et al (2011).

Page 24316 Line 25: The correct reference for the slant column assimilation in TM4, and calculation of stratospheric contribution to the NO2 total column is: Dirksen et al. Journal of Geophysical Research (2011).

We thank the reviewer for pointing this out. Dirksen et al (2011) has now been included in the manuscript, both for the assimilation in TM4 and the troposphere/stratosphere separation.

Page 24319 Line 16-18: Here a reference to Figure 1 should be given.

A reference to Figure 1 has been included here in the revised manuscript.

Figure 2: The sites with zero trend (white colored markers) are very difficult to distinguish. Perhaps change the color of the markers or the color of the background to make these points more apparent.

Based on the reviewer's comment we modified this Figure as follows:

a) *We changed the figure to have a different background color for both land and ocean areas so that the markers with low trend magnitudes are more easily distinguishable.*

b) *We slightly increased the size of the markers.*

Page 24325: The correlations between population growth and NO2 trend for the different regions are very interesting and deserve more discussion. What are the differences between the regions that could drive these distinct clusters? Is it technology? Emissions trends? Trends in regional climate? Measurement artifact? Lamsal et al. Environmental Science and Technology (2013) recently published a similar analysis. How do the results from this work compare?

We significantly expanded this section to discuss in more detail some of the potential drivers of the observed patterns in NO2 trends versus population growth. We also put these results into context by referring to the recent study of Lamsal et al. (2013) on the relationship between NO2 and population density.

Overview of major changes to the manuscript

1. Revised and expanded the introduction to include more references and add more material on Copernicus

2. Significantly expanded the background section to include all the additional references mentioned by the reviewer and many more.

3. Added a new Figure (Figure 2 in the revised manuscript) showing an example of the model fit

4. Added an extensive description of Figure 2 in the revised manuscript

5. Included a discussion of the impact of the quality of model fit on the trend analysis

6. Significantly modified Figure 4 (Figure 5 in the revised manuscript) to include more panels showing additional information on the model fit residuals as well as the time series of an index of economic health

7. Included a detailed description of the additional panels and other aspects of new Figure 5

8. Included a discussion of the relationship between megacity NO2 trends and economic activity

9. Significantly expanded the discussion of former Figure 7 (Figure 8 in the revised manuscript) to explain in more detail the patterns found in this analysis and discuss potential reasons for the observed behavior.

10. Added additional material in the conclusion to give a broader outlook and discuss the relevance of the study for Copernicus

Manuscript prepared for Atmos. Chem. Phys. Discuss.
with version 2014/05/30 6.91 Copernicus papers of the LaTeX class copernicus.cls.
Date: 21 December 2014

Recent satellite-based trends of tropospheric nitrogen dioxide over large urban agglomerations worldwide

P. Schneider[1], W. A. Lahoz[1], and R. van der A[2]

[1]NILU – Norwegian Institute for Air Research, P.O. Box 100, 2027 Kjeller, Norway
[2]Royal Netherlands Meteorological Institute (KNMI), P.O. Box 201, 3730 AE De Bilt, the Netherlands

Correspondence to: P. Schneider (ps@nilu.no)

Abstract

Trends in tropospheric nitrogen dioxide (NO_2) ~~concentrations~~ columns over 66 large urban agglomerations worldwide have been computed using data from the SCanning Imaging Absorption spectroMeter for Atmospheric CHartographY (SCIAMACHY) instrument onboard the Envisat platform for the period August 2002 to March 2012. A seasonal model including a linear trend was fitted to the satellite-based time series over each site. The results indicate distinct spatial patterns in trends. While agglomerations in Europe, North America, and some locations in East Asia/Oceania show decreasing tropospheric NO_2 levels on the order of $-5\,\%\,\mathrm{yr}^{-1}$, rapidly increasing levels of tropospheric NO_2 are found for agglomerations in large parts of Asia, Africa, and South America. The site with the most rapidly increasing absolute levels of tropospheric NO_2 was found to be Tianjin in China with a trend ~~value~~ of $3.04(\pm0.47)\times10^{15}\,\mathrm{molecules\,cm^{-2}\,yr^{-1}}$, whereas the site with the most rapidly increasing relative trend was Kabul in Afghanistan with $14.3(\pm2.2)\,\%\,\mathrm{yr}^{-1}$. In total, 34 sites exhibited increasing trends of tropospheric NO_2 throughout the study period, 24 of which were found to be statistically significant. A total of 32 sites showed decreasing levels of tropospheric NO_2 during the study period, of which 20 sites did so at statistically significant magnitudes. Overall, going beyond the relatively small set of megacities investigated previously, this study provides the first consistent analysis of recent changes in tropospheric NO_2 levels over most large urban agglomerations worldwide, and indicates that changes in urban NO_2 levels are subject to substantial regional differences as well as influenced by economic and demographic factors.

1 Introduction

More than half of the world's population now lives in urban areas. Megacities, i.e. cities with more than 10 million inhabitants, as well as other large urban agglomerations have seen rapid growth over the last decades and this trend is expected to continue in the near future (United Nations, 2012a). The number of megacities is expected to rise from currently 23 to a total of 37 megacities in the year 2025 (Zhu et al., 2012). Such large urban agglomerations exhibit intensive human activities and high levels of energy consumption. This leads to ~~strongly increased~~ very high emissions of a wide variety of air pollutants and greenhouse gases, severely affecting both air quality and climate (Mage et al., 1996; Mayer, 1999; Fenger, 1999; Molina and Molina, 2004; Molina et al., 2004; Gurjar et al., 2008; Chan and Yao, 2008; Monks et al., 2009; Gurjar et al., 2010; Baklanov et al., 2010; Parrish et al., 2011; Kanakidou et al., 2011; Cassiani et al., 2013).

Nitrogen dioxide (NO_2) is one of the major air pollutants and is strongly related to population density (Lamsal et al., 2013) . As such it is a significant environmental issue in many large urban agglomerations ~~(Schneider and van der A, 2012; Lamsal et al., 2013; Hilboll et al., 2013) .~~ (Schneider and van der A, 2012; Liu and Zhu, 2013; Hilboll et al., 2013; Guerreiro et al., 2014) . NO_2, which is primarily emitted by transportation, industry, and domestic heating, is associated with health issues such as airway inflammation and reductions in lung function (World Health Organization, 2013) . However, station observations of NO_2 are relatively rare on a global scale, and in particular in developing countries, and thus are not able to provide a global and spatially continuous perspective. Even in areas with relatively large numbers of air quality monitoring stations such as in Europe and the United States, the station density is often quite low. Satellite observations on the other hand offer a unique opportunity for studying the ~~spatial and~~ continuous spatial patterns and the temporal dynamics of the constituents affecting air quality in general (Martin, 2008; Burrows et al., 2011; Lahoz et al., 2012; Duncan et al., 2014) and of tropospheric NO_2 ~~(Richter et al., 2005; van der A et al., 2008; Schneider and van der A, 2012; Hilboll et al~~ particular (Richter et al., 2005; Martin, 2008; van der A et al., 2008; Zhou et al., 2012; Castellanos an

Furthermore, satellite observations of atmospheric composition are a very important part of operational chemical weather forecasting as it is for example carried out by the Copernicus Atmosphere Monitoring Service (http://atmosphere.copernicus.eu/), which uses data assimilation techniques (Lahoz and Schneider, 2014) to make the best use of the satellite information of atmospheric composition (Flemming et al., 2009; Inness et al., 2013). The Copernicus Atmosphere Monitoring Service is being developed within the framework of a series of EU-funded research projects, the latest of them being the Monitoring Atmospheric Composition and Climate

– Interim Implementation (MACC-II). Within the MACC-II project, a subproject on input data (OBS) organizes, structures, and evaluates input data ~~.~~related to the Copernicus Programme.

As part of this work, the feasibility of using SCanning Imaging Absorption spectroMeter for Atmospheric CartograpHY (SCIAMACHY) data for estimating trends in tropospheric NO_2 was investigated and is reported on here. While SCIAMACHY is not operational anymore and thus does not contribute to the Copernicus Atmosphere Monitoring Service at this point, other existing instruments such as the Global Ozone Monitoring Experiment-2 (GOME-2) (Callies et al., 2000) and the Ozone Monitoring Instrument (OMI) (Levelt et al., 2006) do so, and the presented methodology can be readily linked to these. Furthermore, future Copernicus satellites such as Sentinel-5p, Sentinel-5, and later on the geostationary Sentinel-4 will carry on the existing NO_2 record provided by SCIAMACHY and other instruments. It is therefore important to discuss the methodology and results obtained for a predecessor instrument, as they will be just as applicable and relevant for the successor instruments funded within the framework of the Copernicus programme. Furthermore, there is a strong link between trends in satellite-based NO_2 columns and changes in nitrogen oxides (NO_x) emissions, which in turn have an important effect on the quality of the results provided by modelling systems for atmospheric composition such as the Copernicus Atmospheric Monitoring Service.

Going beyond trends determined over actual megacities as done in previous studies (Schneider and van der A, 2012; Hilboll et al., 2013), we present here the first detailed satellite-based global analysis of tropospheric NO_2 trends for a significantly expanded set of of large urban agglomerations worldwide. The trends are derived from a consistent and homogeneous satellite time series for the period from August 2002 through March 2012, making use of the full archive of SCIAMACHY data.

The manuscript is structured as follows: ~~Sect.~~Section 2 summarizes the current state of knowledge with respect to global and regional satellite-based NO_2 trend analysis. Section 3 describes the datasets used in this study and introduces the methodology applied for calculating the trends. Section 4 subsequently presents the results, including a full overview of the derived trends and statistics for all sites, a discussion of large-scale spatial patterns in trends, an analysis of a global average time series, a discussion of the impact of the time series extraction methodology, and finally a discussion of the relationship between NO_2 trends and population growth. Section 5 ~~then~~ provides a summary and conclusions.

2 Background

Spaceborne observations of NO_2 have been carried out since 1995 when the Global Ozone Monitoring Experiment (GOME) instrument was launched on the European ~~ERS-1~~ ERS-2 platform. Since then, several studies have investigated temporal trends in tropospheric NO_2 provided by spaceborne platforms. Richter et al. (2005) were the first to study space-based NO_2 trends and provided a trend analysis based primarily on GOME NO_2 data over China. Later on, van der A et al. (2006) and van der A et al. (2008) combined data from the GOME and the SCIAMACHY instrument and provided a trend analysis focused on China and over the entire globe, respectively. A combination of GOME and SCIAMACHY data was also used by Ghude et al. (2009) for studying regional trends in tropospheric NO_2. Using a similar methodology, NO_2 trends over emission hotspots in India were further studied by Ghude et al. (2008). Hayn et al. (2009) used generalized additive models to study spatio-temporal patterns in tropospheric NO_2 columns derived from GOME data between 1996 and 2001. Summertime trends in European NO_x emissions were studied by Konovalov et al. (2008) using a combination of GOME, SCIAMACHY, and a continental-scale air quality model. The methodology was later extended to study non-linear NO_2 and NO_x trends for several urban agglomerations in Europe and Asia, using a method based on a probabilistic approach and artificial neural networks (Konovalov et al., 2010). The same combination of satellite instruments was further used by Kim et al. (2006) to quantify decreases in NO_x emissions over US power plants. Russell et al. (2012) studied the effect of emission control measures and the impact of the economic recession in the United States using OMI data. De Ruyter de Wildt et al. (2012) further investigated trends of tropospheric NO_2 over some of the major shipping lanes in the world. Studies focusing on changes in tropospheric NO_2 levels over individual megacities have also been carried out. For example, using data from multiple satellite instruments, Vrekoussis et al. (2013) studied the impact of the economic crisis on the megacity of Athens, Greece. Furthermore, Sitnov (2011) studied OMI-based NO_2 column trends between 2004 and 2009 over the megacity of Moscow, Russia. Constantin et al. (2013) studied time series of tropospheric NO_2 from multiple satellite instruments over several locations in Romania. Ionov (2010) investigated the trend in tropospheric NO_2 column over St. Petersburg, Russia, using a combination of GOME, SCIAMACHY, and OMI data and found a linear increase of approximately 4 % per year. SCIAMACHY-based NO_2 column trends over four large urban agglomerations in India for the period 2004 through 2010 have further been studied by Meena et al. (2012) .

In recent years, spatial patterns and temporal changes in tropospheric NO_2 columns over Europe have been studied in great detail. Based on the work by Hayn et al. (2009) , Zhou et al. (2012) used a generalized additive model together with 6 years of OMI data to study factors influencing the variability of NO_2 columns. They found consistent and significant negative trends mostly in areas of anthropogenic sources over Western Europe and isolated and scattered positive trends in Eastern Europe, which is in agreement with many other studies, such as for example, Schneider and van der A (2012) . Castellanos and Boersma (2012) studied the changes in OMI-based NO_2 columns between 2004 and 2010 over Europe. They found substantial reductions in NO_2 in many parts of Europe, which they attribute in part to European NO_x emission controls and in part to temporary emissions reductions due to the 2008-2009 global economic recession. Using OMI-derived tropospheric columns for NO_2 in conjunction with the chemistry transport model LOTOS-EUROS, Curier et al. (2014) studied trends in NO_x emissions over Europe. Similarly to other studies they found significant negative trends of 5-6 % yr^{-1} in highly industrialized regions of Europe, with the strongest reductions in Northern Spain and the Po Valley.

Schneider and van der A (2012) made use of a homogeneous 9 year time series acquired by the SCIAMACHY instrument and provided the first single-sensor global trend analysis of NO_2, thus avoiding the merging of datasets with substantially different spatial resolution and possible inter-sensor calibration issues. They further analyzed trends over some of the major megacities but did not provide much detail on this issue. For this study we follow the approach suggested by Schneider and van der A (2012) and use data from the SCIAMACHY instrument~~, however~~.

However in contrast to Schneider and van der A (2012) we use the full SCIAMACHY archive and an improved version of the satellite data product. The chosen approach has the advantage of providing very homogeneous time series and therefore highly reliable trends. Combining data from multiple instruments generally requires either resampling to a coarser-resolution grid in order to eliminate the impact of different spatial resolutions (van der A et al., 2006, 2008) or involves schemes for homogenizing the datasets using resolution correction factors (Konovalov et al., 2006; Hilboll et al., 2013) or empirical statistical approaches taking into account level-shift (Mieruch et al., 2008; Hilboll et al., 2013). Although significant progress has been made in techniques on combining data from multiple instruments (Hilboll et al., 2013), computing trends from homogeneous time series based on a single instrument still has the advantage that the computed trends are very likely to be real geophysical trends and are guaranteed not to be affected by different characteristics between instruments.

3 Data and methodology

The data and methodology used here are largely consistent with those used previously in Schneider and van der A (2012). However, there are a few important novel aspects to this work: (a) the primary focus of the study lies on large urban agglomerations (b) the length of the time series has now been expanded to include the entire available archive of SCIAMACHY data ranging from August 2002 to March 2012 (c) a new and improved version of the NO_2 retrieval algorithm (v2.3) (Boersma et al., 2004) has been used, and (d) compared to previous studies the list of large urban agglomerations has been significantly expanded and the resulting trends are studied in more detail.

3.1 Satellite data

Data from the SCIAMACHY instrument onboard the European Space Agency's Envisat platform was used in this study as it provides a homogeneous 10 year time series of global tropospheric NO_2 observations (Bovensmann et al., 1999; Gottwald et al., 2011). SCIAMACHY is a hyperspectral UV/VIS/NIR passive ~~imaging~~ grating spectrometer observing the wavelength range of 214–2386 nm. The entire archive of SCIAMACHY NO_2 data was used (see Fig. 1). The record starts in August 2002 and ends in early April 2012 due to the loss of communication with the Envisat platform. The SCIAMACHY data product of monthly mean tropospheric NO_2 that was used here was processed ~~by KNMI~~ using a combined retrieval/assimilation approach ~~(Boersma et al., 2004)~~ (Boersma et al., 2004; Dirksen et al., 2011) and acquired from the website of the Tropospheric Emission Monitoring Internet Service (TEMIS) (http://temis.nl/). The original satellite retrievals are regridded on a regular 0.25 degree $\times$ 0.25 degree grid by averaging the satellite observations weighted by the size of the overlapping surface area.

The product is derived in a three step approach consisting of (a) Differential Optical Absorption Spectroscopy (DOAS) retrieval of the slant column, (b) a separation of the tropospheric and stratospheric contribution (Dirksen et al., 2011) based on the TM4 chemical transport model (Dentener et al., 2003; Boersma et al., 2007), and (c) conversion of the slant column densities (SCD) into vertical column densities (VCD) using a calculated air mass factor (AMF). While the retrieval in general considers all cloud radiance fractions, the monthly means are calculated only from data with cloud radiance fractions of less than 50 %. The NO_2 product is provided on a global grid of 0.25 degree by 0.25 degree spatial resolution. Version 2.3 of the product was used here. In addition to the major improvements to the retrieval algorithm introduced with version 2.0 (Boersma et al. (2011), and summarized in Schneider and van der A, 2012), version 2.3 further improved the algorithm by correcting some minor retrieval errors. Further details on the specific retrieval methodology can be found in Boersma et al. (2004), Boersma et al. (2007), and Boersma et al. (2011), as well as on the TEMIS website~~()~~.

NO_2 retrievals from SCIAMACHY have been validated in numerous studies, e.g. by Heue et al. (2005) using Airbone Multi-Axis Differential Optical Absorption Spectroscopy observations, by Boersma et al. (2009) using in situ surface observations in Israel, and by Irie et al. (2012) using inter-comparison techniques with NO_2 products derived from other satellite ~~instrument~~ instruments as well as Multi-Axis Differential Optical Absorption Spectroscopy (MAX-DOAS) observations in Japan and China. The ~~latter~~ last one showed that SCIAMACHY-based tropospheric NO_2 columns were accurate with a -5 % bias and standard deviation of

$\pm 14\,\%$. The impact of topography on SCIAMACHY NO_2 retrievals was investigated by Schaub et al. (2007) who found errors of up to $40\,\%$ over very complex terrain. Blond et al. (2007) intercompared SCIAMACHY-based NO_2 retrievals with in situ station observations over Europe and found biases of less than $5\,\%$ and $20\,\%$ for annual and seasonal averages, respectively.

3.2 Site selection

The large urban agglomerations studied here were selected primarily based on population size as given by United Nations (2012b). All "true" megacities, i.e. cities with a population of greater than 10 million inhabitants, were included. In addition, most urban agglomerations with a population of more than 5 million as well as some special-interest sites with slightly less than 5 million inhabitants were also considered. Such ~~special interest-sites~~ special-interest sites were defined on a case by case basis primarily based on properties such as rapid population growth and/or known air quality issues, characteristics as a hotspot in an otherwise unpolluted region, or in order to ~~support balancing the spatial~~ obtain a reasonably balanced distribution of study sites ~~globally~~over the globe.

Overall, 66 large urban agglomerations were identified for the analysis. Of those, seven were located in Africa, fifteen in East Asia, seven in Europe, ten in North America, two in Oceania, six in South America, nine in South Asia, four in South-East Asia, and five in West Asia. A full list of the studied sites including additional information about their ~~exact~~ location and their estimated population is given in Table 1.

3.3 Trend analysis

At each of the sites identified based on the methodology described in Sect. 3.2, time series of mean monthly tropospheric NO_2 were extracted from the full SCIAMACHY archive between August 2002 and March 2012. Subsequently a ~~statistic~~ statistical model was fitted to the time series over each site. The monthly average NO_2 tropospheric column C_t at time t (in months) was modeled following Weatherhead et al. (1998) and Schneider and van der A (2012) as

$$C_t = \mu + S_t + \frac{1}{12}\omega t + R_t \tag{1}$$

where μ is a constant, S_t is a seasonal component, which is a assumed to be constant in time, ω is a linear trend and R_t is the residual variability. The seasonal component S_t is modeled as

$$S_t = \sum_{j=1}^{4}\left[\beta_{1,j}\sin\left(\frac{2\pi jt}{12}\right) + \beta_{2,j}\cos\left(\frac{2\pi jt}{12}\right)\right] \tag{2}$$

where $\beta_{1,1}$ through $\beta_{2,4}$ are coefficients of the fit. The residual variability R_t is assumed to be autoregressive of order 1 and was modeled as

$$R_t = \phi R_{t-1} + \epsilon_t \tag{3}$$

where ϕ is the first order autocorrelation and ϵ is a random error component.

Based on the work by Tiao et al. (1990) and Weatherhead et al. (1998) and following the ~~methdology~~ methodology described in Schneider and van der A (2012), the significance of the trend was calculated such that the trend ω is considered as significant with a 95 % confidence if

$$|\omega/\sigma_\omega| > t_\omega \tag{4}$$

where σ_ω is the uncertainty of the trend and t_ω is the value of the Student's t distribution for a significance level of $\alpha = 0.05$ and the degrees of freedom given for the time series (Santer et al., 2000).

The trend uncertainty σ_ω is computed following Weatherhead et al. (1998) and Schneider and van der A (2012) as

$$\sigma_\omega = \left[\frac{\sigma_r}{n^{3/2}}\sqrt{\frac{1+\phi}{1-\phi}}\right] \tag{5}$$

where σ_r is the standard deviation of the de-trended residuals, n is the number of years with available data, and ϕ is the first-order autocorrelation.

Relative trends ω_{rel} given in % per year are computed from the absolute trends ω_{abs} given in ~~$\times 10^{15}$~~units of molecules $\mathrm{cm}^{-2}\,\mathrm{yr}^{-1}$ with respect to the long-term average tropospheric NO_2 column $\overline{\mathrm{VCD}}_{\mathrm{trop}}$ ~~extracted at each~~ (see Figure 1) as calculated over the original time series at each grid cell. The relative trend ω_{rel} is then calculated at each individual grid cell as

$$\omega_{\mathrm{rel}} = \frac{\omega_{\mathrm{abs}}}{\overline{\mathrm{VCD}}_{\mathrm{trop}}} \cdot 100 \tag{6}$$

This approach of calculating the relative magnitude of the NO_2 trends differs from those taken by previous studies (e.g. van der A et al., 2006, 2008; Hilboll et al., 2013) in that it does not use a single reference year at the beginning of the time series and thus is less sensitive to potential outliers at the gridcell level for the reference year. However, it should be noted that the relative trends reported in this study are therefore not directly comparable to previous studies as they generally show values of lower magnitude.

Figure 2a shows an example of the SCIAMACHY-derived time series of monthly mean tropospheric NO_2 columns together with the statistical model and its linear trend component, which was fitted using the methodology described in this section. In this example, which shows the evolution of the tropospheric NO_2 columns over the city of Baghdad, Iraq, the absolute trend was found to be 0.6 ($\pm$ 0.08) $\times 10^{15}$ molecules $\mathrm{cm}^{-2}\,\mathrm{yr}^{-1}$ and the relative trend with respect to the long-term average tropospheric column levels of NO_2 was found to be 8.5 ($\pm$ 1.2) % per year. Both trends were found to be significant at a 95% confidence. Figure 2b further shows the residuals of the fitted model. The residuals were found to have a mean value of -0.0007 $\times 10^{15}$ molecules cm^{-2} with a standard deviation of 1.7 $\times 10^{15}$ molecules cm^{-2}. The residuals were found to be normally distributed using the Jarque-Bera goodness-of-fit test (Jarque and Bera, 1987) .

In general, we found that the linear trend component of the model, which is the sole purpose of performing the fit of the statistical model in this study, is quite robust even in the presence of occasionally high residuals. However, future work should consider the use of a statistical model that provides the possibility of a variable amplitude in the annual cycle as has been shown for example by Hilboll et al. (2013) . Another potential option are generalized additive models as used by Hayn et al. (2009) and Zhou et al. (2012) . While these methods would improve the model fit and thus lower the magnitude of the residuals, the linear trend component of the model is unlikely to be significantly affected, which is corroborated by the fact that despite differing methodologies most of the relevant studies result in overall very similar magnitudes and spatial patterns of the trends in tropospheric NO_2 columns.

3.4 Data on population growth

Among other factors, the emissions of nitrogen oxides are generally highly dependent on population density (Lamsal et al., 2013). For this reason, the relationship between temporal changes in tropospheric NO_2 and population growth of the urban agglomerations was studied. For this purpose, data on relative population growth by decade in the world's large urban agglomerations with 750 000 inhabitants or more was acquired from the United Nations' World Urbanization Prospects dataset (United Nations, 2012b). Data on population growth was available for the period 2000 to 2010 which agrees very closely with the study period of 2002 to 2012 used here and is thus considered to be suitable for comparison.

4 Results and discussion

4.1 Global trends

Figure 3 shows a global map of the computed trends in tropospheric NO_2 over all studied large urban agglomerations. The overarching spatial patterns visible in the map indicate large-scale decreasing NO_2 levels over all study sites in North America, Europe, Australia and Japan, whereas moderately to rapidly increasing trends can be observed throughout China, South Asia, as well as most of Africa and South America.

A total number of 66 large urban agglomerations were analyzed. Overall, a majority of the studied sites (44 out of 66) exhibited trends that are statistically significant at the 95 % level. In total, 34 sites exhibited increasing trends of tropospheric NO_2 throughout the study period, 24 of which were found to be statistically significant. A total of 32 sites showed decreasing levels of tropospheric NO_2 during the study period, of which 20 sites did so at statistically significant magnitudes. It should be noted that in this study we compute trends of tropospheric NO_2 ~~concentrations~~columns, which differ from the actual emissions. Despite the short ~~life time~~ lifetime of NO_x, the NO_2 concentration field develops a smooth spatial pattern roughly resembling a Gaussian distribution over the emission source, i.e. the city. However, the long-term trends will remain the same regardless of the spatial pattern in the concentration field resembling more a Gaussian or a point source.

Figure 4 shows histograms of absolute and relative trends in tropospheric NO_2 over all the large urban agglomerations studied. The majority of absolute trends falls into the range of ~~-1×10^{15} to 0.5×10~~^{15}-1 $\times10^{15}$ molecules $cm^{-2}\,yr^{-1}$ to 0.5 $\times10^{15}$ molecules $cm^{-2}\,yr^{-1}$, but a few urban agglomerations show even more rapidly decreasing or increasing trends. Most of the relative trends fall into the range between -5 and $6\,\%\,yr^{-1}$, but several of the Asian sites exceed this range with values greater than $6\,\%\,yr^{-1}$.

The overall extreme values in trends are compiled for clarity and given in Table 2. All of these trends are statistically significant at the 95 % level. The maximum value values both in absolute and relative terms were found for megacities in Asia, whereas the most rapid absolute and relative decreases were both found for cities in the United States.

It should be noted that among the "true" megacities, i.e. urban agglomerations with a population of greater than 10 million inhabitants, the city of Dhaka in Bangladesh is the site with the most rapidly increasing largest relative trend with an increase in tropospheric NO_2 levels of $10.3\,\%\,yr^{-1}$ for the period studied here. This is consistent with the multi-instrument trend results reported by Hilboll et al. (2013), although the actual relative trend values differ due to the use of a different methodology for calculating the relative trends (using a single reference year in Hilboll et al. (2013) vs. versus the long-term mean in Schneider and van der A (2012) and this study).

Table 3 shows the absolute and relative trends derived from the entire 2002 to 2012 SCIAMACHY archive for all megacities and large urban agglomerations. For each site the estimated trend uncertainties are also included. The 6 sites with the most rapidly increasing tropospheric NO_2 levels in absolute terms and in fact all sites with absolute trends exceeding 1×10^{15} molecules $cm^{-2}\,yr^{-1}$ all are located in China. In addition to Kabul, three more sites exceed relative trends of $10\,\%\,yr^{-1}$, namely Nairobi, Dhaka, and Chongqing.

4.2 Temporal analysis

Figure 5(top) a shows the average monthly time series computed over all study sites. While the typical seasonal cycle for NO_2 is quite obvious can be seen in the monthly data, no clear linear trend is visible from that data. This is due to the fact that the time series represents an average over all worldwide megacities and large urban agglomerations with widely varying characteristics, including both rapidly increasing trends in Asia as well as decreasing NO_2 levels in North America and Europe. Figure 5a also shows the fitted statistical model used to deseasonalize the time series. Figure 5b shows the correponding residuals, which in the majority of cases have absolute values of less than 2×10^{15}

$$\text{molecules}\,\text{cm}^{-2}\,\text{yr}^{-1}.$$

In order to To better highlight the overall signal contained in the global monthly time series, Fig. 5(bottom) Figure 5c further shows the 12-month moving average of the deseasonalized monthly time series. The most obvious characteristic in this plot is a significant drop in concentrations tropospheric NO_2 levels throughout the year 2008, which then continuous continue at low levels throughout 2009 and 2010, after which the levels recover again slightly until 2011. This feature is most likely related to the worldwide financial crisis, which started in 2008 and had a substantial impact on the global economy during this period. This result provides a global perspective to supplement previous studies that looked in detail at tropospheric NO_2 concentrations columns as a proxy for the economic downturn over a single megacity (Vrekoussis et al., 2013) or provided regional studies about the same topic (Russell et al., 2012; Castellanos and Boersma, 2012; De Ruyter de Wildt et al., 2012).

Figure 5c also indicates an increase in tropospheric NO_2 levels from late 2003 through early 2004. The reason for this behavior is not as obvious. To better understand this feature,

Figure 5d shows a monthly-averaged time series of the Economic Cycle Research Institute (ECRI) leading weekly economic index (https://www.businesscycle.com/ecri-reports-indexes/all-indexes). While this index is primarily intended as an indicator of the economic outlook for the United States (higher values indicate a more positive outlook), we use it here as a proxy for the global economic situation. Both the increase in 2003/2004 as well as the rapid drop in 2008 can be seen in both datasets, suggesting a link between the NO_2 levels over large urban agglomerations and the economic situation. It should be noted that other features such as the small temporary decrease in NO_2 levels in 2006 (Figure 5c), or the moderate rise of the NO_2 levels in 2010, are not reflected as clearly by the economic index. However, the latter could be interpreted as a slightly delayed response, keeping in mind that the NO_2 levels shown in Figure 5c are global averages whereas the economic index shown in Figure 5d is for the United States. Overall, these results indicate that the global average NO_2 levels over major urban agglomerations reflect large-scale changes in the global economic situation that happen over a relatively short timeframe.

In addition to the global time series given in Fig. 5, average time series were also studied at the regional level. Figure 6 shows the interannual variability of tropospheric NO_2 over all studied megacities and urban agglomerations, averaged by region. To facilitate an easier comparison between regions, the time series are given as averaged relative anomalies from the long-term mean at each site. The large-scale spatial patterns discussed previously are confirmed in this figure, with the urban agglomerations in Europe and North America exhibiting substantial decreases in NO_2, and the regions of South Asia, West Asia, and Africa showing rapid increases over the only 9 year period. North American agglomerations show a particularly drastic strong decrease in NO_2 after 2005, continuing until the end of the study period. This is likely related to emission reduction measures which have been carried out during this period. In European agglomerations the NO_2 decrease appears to have stopped after 2008. The South Asia region shows the clearest increasing signal as the urban agglomerations located in this area all exhibit positive trends. The averaged time series for East Asia and South America do not show a clear signal because the regions contain agglomerations with both increasing and decreasing NO_2 levels.

4.3 Impact of time series extraction methodology

The methodology by which the time series are extracted from the satellite data can to some extent affect the magnitude of the trends, depending on the spatial homogeneity of the trends patterns in the surroundings of area surrounding each urban agglomeration. In order to study this, time series were extracted from the satellite data using two approaches. The first one only used the grid cell in which the center of the urban agglomeration was located. The second approach used the average value of a 3×3 grid cell array centered on the same location.

Figure 7 illustrates the effect of the size of the averaging region on the resulting absolute and relative trends when the time series are extracted either from a single grid cell (here denoted as $\omega_{\mathrm{abs}(1\times1)}$ and $\omega_{\mathrm{rel}(1\times1)}$), or as the average of a 3×3 grid cell array centered over the study site , (here denoted as $\omega_{\mathrm{abs}(3\times3)}$ and $\omega_{\mathrm{rel}(3\times3)}$) .

The mean difference between the absolute trends, calculated as $\omega_{\mathrm{abs}(1\times1)} - \omega_{\mathrm{abs}(3\times3)}$, from time series derived from a single grid vs. a 3×3 grid cell array was found to be 0.013×10^{15} 0.013×10^{15}

$$\mathrm{molecules\,cm^{-2}\,yr^{-1}} with a\ standard deviation of$$

0.16×10^{15} 0.16×10^{15} molecules $\mathrm{cm^{-2}\,yr^{-1}}$ $and\, an\, a\, root mean squared error (RMSE) of$ 0.16×10^{15} 0.16×10^{15}

$$\mathrm{molecules\,cm^{-2}\,yr^{-1}}.The largest deviation in absolute trends was found for Chengdu, China, wit$$

0.5×10^{15} 0.5×10^{15} molecules $\mathrm{cm^{-2}\,yr^{-1}}$. This is likely related to the specific orography of the region around Chengdu with high mountains surrounding the city to the South, West, and North. As for deviations in relative trends, calculated as $\omega_{\mathrm{rel}(1\times1)} - \omega_{\mathrm{rel}(3\times3)}$, the mean difference was found to be $0.25\,\%\,\mathrm{yr}^{-1}$ with a standard deviation of $1.09\,\%\,\mathrm{yr}^{-1}$ and an RMSE of $1.1\,\%\,\mathrm{yr}^{-1}$. The largest deviation in terms of relative trends was observed for the city of Lagos, Nigeria, with a value of $4.18\,\%\,\mathrm{yr}^{-1}$.

The results above indicate that the two approaches are quite comparable and mostly differ by values that are negligible as compared to the overall magnitude of the trends and their estimated uncertainties. However, for a few cases, such as for example the city of Lagos, the trend difference between the two extraction approaches reaches values that exceed 50 % of the actual trend value and thus can have a significant impact on the results. Obviously, the differences observed here are to a large extent due to variability in the spatial extent of the urban agglomerations and not in all cases a 3×3 grid cell average is warranted. Since columns rather than emissions are studied here, the spatial patterns over a NO_x source such as a megacity will mostly appear spatially smoothed, which limits the effect of spatial gradients. As such, the spatial variability and the area over which the trends are computed will generally only play a significant role for agglomerations with a very large spatial extent as for example the greater Los Angeles area, which covers substantially more than 9 grid cells of the 0.25 degree $\times$ 0.25 degree spatial resolution NO_2 product used here .

Therefore, while the 3×3 grid cell array approach has the advantage of providing more valid monthly mean values and thus time series which result in a slightly better model fit, it was decided here to use the single grid cell approach for extracting the time series as it ensures that all sites are well represented in the time series, independent of the spatial shape and size of the city. For agglomerations with a very large spatial extent, such as Los Angeles, future work could explore the option of calculating the trends over the entire area covered by each site, for example as given by polygon outlines.

4.4 NO_2 trends and population growth

NO_2 concentrations are generally closely linked to population density (Lamsal et al., 2013). For this reason, the worldwide trends in tropospheric NO_2 columns obtained from SCIAMACHY for the studied large urban agglomerations were compared with data on population growth at the same sites.

Figure 8 shows the relationship between population growth for the period 2000 to 2010 and satellite-derived trends in tropospheric NO_2 for the period 2002 to 2012, classified by region. The results show distinctly surprisingly different behavior for each region. A linear relationship between NO_2 trend and population growth can be seen for large urban agglomerations in Europe and South Asia.

In Europe the relationship roughly follows the regression equation $\omega_{rel} = -3.8 + 1.6 \cdot \mathrm{PG}$, where ω_{rel} is the SCIAMACHY-derived relative trend in tropospheric NO_2 concentration in % yr^{-1} and PG is the population growth over the 2000 through 2010 period given in %. This relationship has an a coefficient of determination of R^2 value of = 0.74.

Similarly, in South Asia the relationship roughly follows the regression equation $\omega_{rel} = -1.7 + 2.1 \cdot \mathrm{PG}$ with an R^2 value of 0.72. It should be noted, however, that both relationships are based on a relatively small sample size of $N = 7$ and $N = 10$ for Europe and South Asia, respectively.

In other regions besides Europe and South Asia, no obvious linear relationships are visible in Fig. Figure 8, although distinct patterns clearly do emerge. For East Asia, a clear division between Chinese and primarily Japanese/Korean agglomerations (with the exception of Hong Kong) is visible, with the former exhibiting both strong population growth and rapid increases in tropospheric NO_2, whereas the latter show very weak population growth (or even -loss loss) and decreases in tropospheric NO_2 between 0 and $-5\,\%\,yr^{-1}$. A special case are the two Chinese megacities of Guanghzou and Shenzhen which, despite having strong population growth, exhibit decreasing levels of NO_2, most likely due to politically motivated emission reduction measures in this area emission reductions linked to changes in local legislation .

Only 5 sites were available in West Asia and no clear pattern or relationship can be inferred. Baghdad has a surprisingly rapid increase in tropospheric NO_2 levels of $9\,\%\,yr^{-1}$ given its relatively low population growth of only around $1\,\%$.

Megacities and large urban agglomerations in North and South America clearly fall into one of two main clusters. North American agglomerations exhibit moderate population growth between 0 and $4\,\%$ for the 2000 to 2010 period, however they all clearly show NO_2 decreases between -5 and $-10\,\%\,yr^{-1}$. The exception here is Mexico City, which only exhibits very minor NO_2 decreases. The other cluster is formed by South American agglomerations which exhibit mostly similar rates of population growth but, with the exception of Bogota, show constant or increasing tropospheric NO_2 levels.

Finally, African megacities and agglomerations do not indicate a strong relationship between population growth and NO_2 trend or other patterns. With most sites except Cairo exhibiting population growth rates greater than 2 % for 2000–2010, Johannesburg is the only African site with decreasing tropospheric NO_2 levels. All other sites exhibit growth in the tropospheric NO_2 concentrations columns, which in the case of Nairobi reach very high levels of over 13 % yr^{-1}.

These results complement a recent study by Lamsal et al. (2013) who investigated the relationship between urban surface concentrations of NO_2, which were estimated from satellite and model data, and population density. They found significant correlations between these two parameters for a power law scaling function. The relationship was significant for all studied regions with approximately similar correlation strengths, however the slope of the power law regression varied between the regions and for China in particular. Our approach differs from that of Lamsal et al. (2013) in several aspects. Most importantly we study changes in NO_2 over time and do not compare these with population density but with the change in overall population during the study period. As such, our study focuses more on investigating to what extent population changes in urban agglomerations are mirrored by changes in tropospheric NO_2 levels.

It is not entirely obvious what causes the various patterns in the different regions shown in Figure 8. Both Europe and South Asia show linear relationships as one might initially expect, with population growth explaining more rapidly increasing (or less rapidly decreasing) levels in tropospheric NO_2 columns. However, the other areas do not show such a straightforward relationship and rather appear to reflect regional differences in industrial and demographic development. In some regions, for example for the agglomerations in China and West Asia, Figure 8 even appears to indicate a weak inverse relationship, i.e. lower trends in NO_2 columns with increasing population growth. This is somewhat counterintuitive but could to some extent reflect the fact that more developed and industrialized agglomerations, which already might have some legislative emission control strategies in place and thus exhibit only weakly increasing NO_2 levels, could be more appealing to rural migrant workers due to better employment opportunities, thus explaining the higher population growth. Given the very low sample sizes for the individual regions with N < 10 in most cases and the resulting uncertainty in trend patterns, however, this is mostly speculation and any interpretation going beyond this discussion is challenging. Additional research on this issue, possibly using a significantly increased number of study sites and a more detailed and targeted analysis will be necessary to better understand the underlying causes for the observed patterns.

5 Conclusions

Megacities and other large urban agglomerations are major hotspots for air pollution. Given the substantial global population growth and the strong tendency towards urbanization, this problem will be exacerbated in future decades. Here we present an overview of recent changes and trends in satellite-derived tropospheric NO_2 concentrations columns over 66 of the largest urban agglomerations worldwide. The trends were derived by fitting a statistical model including a linear trend and a seasonal component to time series extracted from the full SCIAMACHY satellite data archive for the period August 2002 to March 2012.

Overall, 45 44 of the 66 study sites showed statistically significant trends (either positive or negative) at the 95 % level. Of those In total , 34 sites exhibited increasing trends levels of tropospheric NO_2 throughout the study period, 24 of which were found to be statistically significant. In addition, 32 sites showed decreasing levels of tropospheric NO_2 during the study period, of which 20 sites did so at statistically significant magnitudes. The most extreme increasing absolute and relative values in trends during the study period were found for two Asian sites (Tianjin in China and Kabul in Afghanistan, respectively), whereas the most rapidly decreasing absolute and relative trends were observed for two sites in North America (Los Angeles and Boston, respectively).

Spatial patterns in worldwide trends for megacities and large urban agglomerations were studied. Similarly to previous studies investigating global tropospheric NO_2 trends (van der A et al., 2008; Schneider and van der A, 2012; Hilboll et al., 2013), the characteristics characteristic patterns for trends over urban agglomerations include a spatially homogeneous reduction in concentrations tropospheric NO_2 columns over both Europe and North America on the level of around $-5\,\%\,\mathrm{yr}^{-1}$, and moderately to rapidly increasing concentrations tropospheric column amounts of NO_2 over large parts of Asia as well as Africa and South America, reaching relative trend magnitudes as high as $15\,\%\,\mathrm{yr}^{-1}$.

In addition to spatial patterns, the time series over the urban agglomerations were studied both at the global and regional level. At the global level no strong overall trends were observed but a signal of the 2008/2009 economical crisis was identified. The analysis of average time series at the regional level confirmed the overall patterns found in the spatial analysis. Finally, the relationship between the satellite-derived NO_2 trends over urban agglomerations and urban population growth was investigated. Clear linear relationships were found for Europe and South Asia, but other regions did not indicate such relationships, although characteristic clusters distinguishing sites in developing vs. developed countries did emerge.

Overall, this study provides what is currently the most comprehensive global overview of recent changes in tropospheric NO_2 levels over large urban agglomerations worldwide. It was carried out using a homogeneous and consistent satellite dataset acquired from a single instrument and processed using a single algorithm, thus providing trends with a high accuracy and free of inter-sensor calibration issues. Trend analysis is one of the most useful applications of satellite data of atmospheric composition and future satellite instruments, for example those to be launched within the framework of the European Copernicus Programme, will continue the NO_2 record provided by SCIAMACHY and other satellite instruments. As such the study of NO_2 trends from predecessor satellite instruments is very relevant for users of NO_2 data from the future Copernicus satellites, both in terms of extending the NO_2 trends and for assessing the quality of NO_2 data from these future satellites.

An important next step with respect to monitoring changes in tropospheric NO_2 from space will be the direct validation of satellite-derived trendsin tropospheric . There are now several stations worldwide providing observations from Multi-Axis Differential Optical Absorption Spectroscopy (ground-based MAX-DOAS) instruments (Hönninger et al., 2004; Irie et al., 2012; Kanaya et al., 2014; Hendrick et al., 2014), providing highly accurate measurements of tropospheric columns of various trace gases. Some of these stations now provide time series of 5 years and more, thus allowing for a direct comparison of satellite-derived trends with trends obtained from a reliable reference source. Such a direct validation will add value to NO_2 trends computed from the various satellite products as it will provide a realistic estimate of the uncertainty involved in such analyses.

Acknowledgements. This work has been partially supported by the MACC-II project funded by the European Union under the Seventh Framework Programme (FP7 THEME [SPA.2011.1.5-02]) under grant agreement n. 283576. Further funding was provided by the Norwegian Space Centre within the SatMonAir-I and SatMonAir-II projects. We gratefully acknowledge the free use of tropospheric NO_2 column data from the SCIAMACHY sensor provided by www.temis.nl.

References

Baklanov, A., Lawrence, M., Pandis, S., Mahura, A., Finardi, S., Moussiopoulos, N., Beekmann, M., Laj, P., Gomes, L., Jaffrezo, J.-L., Borbon, A., Coll, I., Gros, V., Sciare, J., Kukkonen, J., Galmarini, S., Giorgi, F., Grimmond, S., Esau, I., Stohl, A., Denby, B., Wagner, T., Butler, T., Baltensperger, U., Builtjes, P., van den Hout, D., van der Gon, H. D., Collins, B., Schluenzen, H., Kulmala, M., Zilitinkevich, S., Sokhi, R., Friedrich, R., Theloke, J., Kummer, U., Jalkinen, L., Halenka, T., Wiedensholer, A., Pyle, J., and Rossow, W. B.: MEGAPOLI: concept of multi-scale modelling of megacity impact on air quality and climate, Adv. Sci. Res., 4, 115–120, doi:10.5194/asr-4-115-2010, 2010.

Blond, N., Boersma, K. F., Eskes, H. J., van der A, R. J., Van Roozendael, M., De Smedt, I., Bergametti, G., and Vautard, R.: Intercomparison of SCIAMACHY nitrogen dioxide observations, in situ measurements and air quality modeling results over Western Europe, J. Geophys. Res., 112, 1–20, doi:10.1029/2006JD007277, 2007.

Boersma, K. F., Eskes, H. F., and Brinksma, E. J.: Error analysis for tropospheric NO_2 retrieval from space, J. Geophys. Res., 109, D04311, doi:10.1029/2003JD003962, 2004.

Boersma, K. F., Eskes, H. J., Veefkind, J. P., Brinksma, E. J., van der A, R. J., Sneep, M., van den Oord, G. H. J., Levelt, P. F., Stammes, P., Gleason, J. F., and Bucsela, E. J.: Near-real time retrieval of tropospheric NO_2 from OMI, Atmos. Chem. Phys., 7, 2103–2118, doi:10.5194/acp-7-2103-2007, 2007.

Boersma, K. F., Jacob, D. J., Trainic, M., Rudich, Y., DeSmedt, I., Dirksen, R., and Eskes, H. J.: Validation of urban NO_2 concentrations and their diurnal and seasonal variations observed from the SCIAMACHY and OMI sensors using in situ surface measurements in Israeli cities, Atmos. Chem. Phys., 9, 3867–3879, doi:10.5194/acp-9-3867-2009, 2009.

Boersma, K. F., Eskes, H. J., Dirksen, R. J., van der A, R. J., Veefkind, J. P., Stammes, P., Huijnen, V., Kleipool, Q. L., Sneep, M., Claas, J., Leitão, J., Richter, A., Zhou, Y., and Brunner, D.: An improved tropospheric NO_2 column retrieval algorithm for the Ozone Monitoring Instrument, Atmos. Meas. Tech., 4, 1905–1928, doi:10.5194/amt-4-1905-2011, 2011.

Bovensmann, H., Burrows, J. P., Buchwitz, M., Frerick, J., Noël, S., Rozanov, V. V., Chance, K. V., and Goede, A. P. H.: SCIAMACHY: Mission Objectives and Measurement Modes, J. Atmos. Sci., 56, 127–150, doi:10.1175/1520-0469(1999)056<0127:SMOAMM>2.0.CO;2, 1999.

Burrows, J. P., Platt, U., and Borrell, P., eds.: The Remote Sensing of Tropospheric Composition from Space , Springer, 2011.

Callies, J., Corpaccioli, E., Eisinger, M., Hahne, A., and Lefebvre, A.: GOME-2 - Metop's Second-Generation Sensor for Operational Ozone Monitoring , ESA Bulletin, 102, 28–36, 2000.

Cassiani, M., Stohl, A., and Eckhardt, S.: The dispersion characteristics of air pollution from the world's megacities, Atmos. Chem. Phys., 13, 9975–9996, doi:10.5194/acp-13-9975-2013, 2013.

Castellanos, P. and Boersma, K. F.: Reductions in nitrogen oxides over Europe driven by environmental policy and economic recession, Scientific Reports, 2, 265, doi:10.1038/srep00265, 2012.

Chan, C. K. and Yao, X.: Air pollution in mega cities in China, Atmos. Environ., 42, 1–42, doi:10.1016/j.atmosenv.2007.09.003, 2008.

Curier, R. L., Kranenburg, R., Segers, A. J. S., Timmermans, R. M. A., and Schaap, M.: Synergistic use of OMI NO2 tropospheric columns and LOTOS-EUROS to evaluate the NOx emission trends across Europe , Remote Sensing of Environment, 149, 58–69, doi:10.1016/j.rse.2014.03.032, http://dx.doi.org/10.1016/j.rse.2014.03.032, 2014.

Constantin, D.-E., Voiculescu, M., and Georgescu, L.: Satellite observations of NO2 trend over Romania. , The Scientific World Journal, pp. 1–10, doi:10.1155/2013/261634, 2013.

De Ruyter de Wildt, M., Eskes, H., and Boersma, K. F.: The global economic cycle and satellite-derived NO_2 trends over shipping lanes, Geophys. Res. Lett., 39, 2–7, doi:10.1029/2011GL049541, 2012.

Dentener, F., van Weele, M., Krol, M., Houweling, S., and van Velthoven, P.: Trends and inter-annual variability of methane emissions derived from 1979-1993 global CTM simulations, Atmos. Chem. Phys., 3, 73–88, doi:10.5194/acp-3-73-2003, 2003.

Dirksen, R. J., Boersma, K. F., Eskes, H. J., Ionov, D. V., Bucsela, E. J., Levelt, P. F., and Kelder, H. M.: Evaluation of stratospheric NO 2 retrieved from the Ozone Monitoring Instrument: Intercomparison, diurnal cycle, and trending , Journal of Geophysical Research, 116, D08 305, doi:10.1029/2010JD014943, http://doi.wiley.com/10.1029/2010JD014943, 2011.

Duncan, B. N., Prados, A. I., Lamsal, L. N., Liu, Y., Streets, D. G., Gupta, P., Hilsenrath, E., Kahn, R. A., Nielsen, J. E., Beyersdorf, A. J., Burton, S. P., Fiore, A. M., Fishman, J., Henze, D. K., Hostetler, C. A., Krotkov, N. A., Lee, P., Lin, M., Pawson, S., Pfister, G., Pickering, K. E., Pierce, R. B., Yoshida, Y., and Ziemba, L. D.: Satellite data of atmospheric pollution for U.S. air quality applications: Examples of applications, summary of data end-user resources, answers to FAQs, and common mistakes to avoid , Atmospheric Environment, 94, 647–662, doi:10.1016/j.atmosenv.2014.05.061, http://linkinghub.elsevier.com/retrieve/pii/S1352231014004270, 2014.

Fenger, J.: Urban air quality, Atmos. Environ., 33, 4877–4900, doi:10.1016/S1352-2310(99)00290-3, 1999.

Flemming, J., Inness, A., Flentje, H., Huijnen, V., Moinat, P., Schultz, M. G., and Stein, O.: Coupling global chemistry transport models to ECMWF's integrated forecast system, Geosci. Model Dev., 2, 253–265, doi:10.5194/gmd-2-253-2009, 2009.

Ghude, S. D., Fadnavis, S., Beig, G., Polade, S. D., and van der A, R. J.: Detection of surface emission hot spots, trends, and seasonal cycle from satellite-retrieved NO_2 over India, J. Geophys. Res., 113, 1–13, doi:10.1029/2007JD009615, 2008.

Ghude, S. D., Van der A, R. J., Beig, G., Fadnavis, S., and Polade, S. D.: Satellite derived trends in NO_2 over the major global hotspot regions during the past decade and their inter-comparison, Environ. Pollut., 157, 1873–1878, doi:10.1016/j.envpol.2009.01.013, 2009.

Gottwald, M., Bovensmann, H., Lichtenberg, G., Noel, S., Bargen, A. von, Slijkhuis, S., Piters, A., Hoogeveen, R., Savigny, C. von, Buchwitz, M., Kokhanovsky, A., Richter, A., Rozanov, A., Holzer-Popp, T., Bramstedt, K., Lambert, J.-C., Skupin, J., Wittrock, F., Schrijver, H., and Burrows, J. P.: SCIAMACHY – Exploring the Changing Earth's Atmosphere, Springer, Dordrecht, the Netherlands, 2011.

Guerreiro, C. B., Foltescu, V., and de Leeuw, F.: Air quality status and trends in Europe , Atmospheric Environment, 98, 376–384, doi:10.1016/j.atmosenv.2014.09.017, http://linkinghub.elsevier.com/retrieve/pii/S1352231014007109, 2014.

Gurjar, B., Butler, T., Lawrence, M., and Lelieveld, J.: Evaluation of emissions and air quality in megacities, Atmos. Environ., 42, 1593–1606, doi:10.1016/j.atmosenv.2007.10.048, 2008.

Gurjar, B., Jain, A., Sharma, A., Agarwal, A., Gupta, P., Nagpure, A. S., and Lelieveld, J.: Human health risks in megacities due to air pollution, Atmos. Environ., 44, 4606–4613, doi:10.1016/j.atmosenv.2010.08.011, 2010.

Hayn, M., Beirle, S., Hamprecht, F. A., Platt, U., Menze, B. H., and Wagner, T.: Analysing spatio-temporal patterns of the global NO2-distribution retrieved from GOME satellite observations using a generalized additive model , Atmospheric Chemistry and Physics, 9, 6459–6477, 2009.

Hendrick, F., Müller, J.-F., Clémer, K., Wang, P., De Mazière, M., Fayt, C., Gielen, C., Hermans, C., Ma, J. Z., Pinardi, G., Stavrakou, T., Vlemmix, T., and Van Roozendael, M.: Four years of ground-based MAX-DOAS observations of HONO and NO_2 in the Beijing area, Atmos. Chem. Phys., 14, 765–781, doi:10.5194/acp-14-765-2014, 2014.

Heue, K.-P., Richter, A., Bruns, M., Burrows, J. P., v. Friedeburg, C., Platt, U., Pundt, I., Wang, P., and Wagner, T.: Validation of SCIAMACHY tropospheric NO_2-columns with AMAXDOAS measurements, Atmos. Chem. Phys., 5, 1039–1051, doi:10.5194/acp-5-1039-2005, 2005.

Hilboll, A., Richter, A., and Burrows, J. P.: Long-term changes of tropospheric NO_2 over megacities derived from multiple satellite instruments, Atmos. Chem. Phys., 13, 4145–4169, doi:10.5194/acp-13-4145-2013, 2013.

Hönninger, G., von Friedeburg, C., and Platt, U.: Multi axis differential optical absorption spectroscopy (MAX-DOAS), Atmos. Chem. Phys., 4, 231–254, doi:10.5194/acp-4-231-2004, 2004.

Inness, A., Baier, F., Benedetti, A., Bouarar, I., Chabrillat, S., Clark, H., Clerbaux, C., Coheur, P., Engelen, R. J., Errera, Q., Flemming, J., George, M., Granier, C., Hadji-Lazaro, J., Huijnen, V., Hurtmans, D., Jones, L., Kaiser, J. W., Kapsomenakis, J., Lefever, K., Leitão, J., Razinger, M., Richter, A., Schultz, M. G., Simmons, A. J., Suttie, M., Stein, O., Thépaut, J.-N., Thouret, V., Vrekoussis, M., Zerefos, C., and the MACC team: The MACC reanalysis: an 8 yr data set of atmospheric composition, Atmos. Chem. Phys., 13, 4073–4109, doi:10.5194/acp-13-4073-2013, 2013.

Ionov, D. V.: Tropospheric NO2 trend over St. Petersburg (Russia) as measured from space , Russian Journal of Earth Sciences, 11, 1–7, doi:10.2205/2010ES000437, http://elpub.wdcb.ru/journals/rjes/doi/2010ES000437.html, 2010.

Irie, H., Boersma, K. F., Kanaya, Y., Takashima, H., Pan, X., and Wang, Z. F.: Quantitative bias estimates for tropospheric NO_2 columns retrieved from SCIAMACHY, OMI, and GOME-2 using a common standard for East Asia, Atmos. Meas. Tech., 5, 2403–2411, doi:10.5194/amt-5-2403-2012, 2012.

Jarque, C. M. and Bera, A. K.: A test for normality of observations and regression residuals , International Statistical Review, 55, 163–172, http://www.jstor.org/stable/1403192, 1987.

Kanakidou, M., Mihalopoulos, N., Kindap, T., Im, U., Vrekoussis, M., Gerasopoulos, E., Dermitzaki, E., Unal, A., Koçak, M., Markakis, K., Melas, D., Kouvarakis, G., Youssef, A. F., Richter, A., Hatzianastassiou, N., Hilboll, A., Ebojie, F., Wittrock, F., von Savigny, C., Burrows, J. P., Ladstaetter-

Weissenmayer, A., and Moubasher, H.: Megacities as hot spots of air pollution in the East Mediterranean, Atmos. Environ., 45, 1223–1235, doi:10.1016/j.atmosenv.2010.11.048, 2011.

Kanaya, Y., Irie, H., Takashima, H., Iwabuchi, H., Akimoto, H., Sudo, K., Gu, M., Chong, J., Kim, Y. J., Lee, H., Li, A., Si, F., Xu, J., Xie, P.-H., Liu, W.-Q., Dzhola, A., Postylyakov, O., Ivanov, V., Grechko, E., Terpugova, S., and Panchenko, M.: Long-term MAX-DOAS network observations of NO_2 in Russia and Asia (MADRAS) during the period 2007–2012: instrumentation, elucidation of climatology, and comparisons with OMI satellite observations and global model simulations, Atmos. Chem. Phys., 14, 7909–7927, doi:10.5194/acp-14-7909-2014, 2014.

Kim, S.-W., Heckel, A., McKeen, S. A., Frost, G. J., Hsie, E.-Y., Trainer, M. K., Richter, A., Burrows, J. P., Peckham, S. E., and Grell, G. A.: Satellite-observed U. S. power plant NO_x emission reductions and their impact on air quality, Geophys. Res. Lett., 33, 1–5, doi:10.1029/2006GL027749, 2006.

Konovalov, I. B., Beekmann, M., Richter, A., and Burrows, J. P.: Inverse modelling of the spatial distribution of NO_x emissions on a continental scale using satellite data, Atmos. Chem. Phys., 6, 1747–1770, doi:10.5194/acp-6-1747-2006, 2006.

Konovalov, I. B., Beekmann, M., Burrows, J. P., and Richter, A.: Satellite measurement based estimates of decadal changes in European nitrogen oxides emissions, Atmos. Chem. Phys., 8, 2623–2641, doi:10.5194/acp-8-2623-2008, 2008.

Konovalov, I. B., Beekmann, M., Richter, A., Burrows, J. P., and Hilboll, A.: Multi-annual changes of NO_x emissions in megacity regions: nonlinear trend analysis of satellite measurement based estimates, Atmos. Chem. Phys., 10, 8481–8498, doi:10.5194/acp-10-8481-2010, 2010.

Lahoz, W. A., Peuch, V.-H., Orphal, J., Atti é, J.-L., Chance, K., Liu, X., Edwards, D., Elbern, H., Flaud, J.-M., Claeyman, M., and Amraoui, L. E.: Monitoring Air Quality from Space: The Case for the Geostationary Platform , Bulletin of the American Meteorological Society, 93, 221–233, doi:10.1175/BAMS-D-11-00045.1, http://journals.ametsoc.org/doi/abs/10.1175/BAMS-D-11-00045.1, 2012.

Lahoz, W. A. and Schneider, P.: Data assimilation: making sense of Earth Observation, Frontiers in Environmental Science, 2, 1–28, doi:10.3389/fenvs.2014.00016, 2014.

Lamsal, L. N., Martin, R. V., Parrish, D. D., and Krotkov, N. A.: Scaling relationship for NO_2 pollution and urban population size: a satellite perspective, Environ. Sci. Technol., 47, 7855–7861, doi:10.1021/es400744g, 2013.

Levelt, P., van den Oord, G., Dobber, M., Malkki, A., Stammes, P., Lundell, J., and Saari, H.: The Ozone Monitoring Instrument , IEEE Transactions on Geoscience and Remote Sensing, 44, 1093–1101, doi:10.1109/TGRS.2006.872333, http://ieeexplore.ieee.org/xpl/freeabs_all.jsp?arnumber=1624590, 2006.

Liu, J. and Zhu, T.: NOx in Chinese Megacities, in: Disposal of Dangerous Chemicals in Urban Areas and Mega Cities, edited by Barnes, I. and Rudziński, K. J., in NATO Science for Peace and Security Series C: Environmental Security, pp. 249–263, Springer Netherlands, Dordrecht, doi:10.1007/978-94-007-5034-0, http://link.springer.com/10.1007/978-94-007-5034-0, 2013.

Mage, D., Ozolins, G., Peterson, P., Webster, A., Orthofer, R., Vandeweerd, V., and Gwynne, M.: Urban air pollution in megacities of the world, Atmos. Environ., 30, 681–686, doi:10.1016/1352-2310(95)00219-7, 1996.

Martin, R. V.: Satellite remote sensing of surface air quality, Atmospheric Environment, 42, 7823–7843, doi:10.1016/j.atmosenv.2008.07.018, http://linkinghub.elsevier.com/retrieve/pii/S1352231008006328, 2008.

Mayer, H.: Air pollution in cities, Atmos. Environ., 33, 4029–4037, doi:10.1016/S1352-2310(99)00144-2, 1999.

Meena, G. S., Patil, S. D., Manoj, M. G., and Devara, P. C. S.: Tropospheric NO2 variability over the metropolitan cities and hill stations of India, Natural Hazards, 65, 723–737, doi:10.1007/s11069-012-0392-1, http://link.springer.com/10.1007/s11069-012-0392-1, 2012.

Mieruch, S., Noël, S., Bovensmann, H., and Burrows, J. P.: Analysis of global water vapour trends from satellite measurements in the visible spectral range, Atmos. Chem. Phys., 8, 491–504, doi:10.5194/acp-8-491-2008, 2008.

Molina, L. T., Molina, M. J., Slott, R. S., Kolb, C. E., Gbor, P. K., Meng, F., Singh, R. B., Galvez, O., Sloan, J. J., Anderson, W. P., Tang, X., Hu, M., Xie, S., Shao, M., Zhu, T., Zhang, Y., Gurjar, B. R., Artaxo, P. E., Oyola, P., Gramsch, E., Hidalgo, D., and Gertler, A. W.: Air quality in selected megacities, J. Air Waste Manage., 54, 1–73, doi:10.1080/10473289.2004.10471015, 2004.

Molina, M. J. and Molina, L. T.: Megacities and atmospheric pollution, J. Air Waste Manage., 54, 644–680, doi:10.1080/10473289.2004.10470936, 2004.

Monks, P., Granier, C., Fuzzi, S., Stohl, A., Williams, M., Akimoto, H., Amann, M., Baklanov, A., Baltensperger, U., Bey, I., Blake, N., Blake, R., Carslaw, K., Cooper, O., Dentener, F., Fowler, D., Fragkou, E., Frost, G., Generoso, S., Ginoux, P., Grewe, V., Guenther, A., Hansson, H., Henne, S., Hjorth, J., Hofzumahaus, A., Huntrieser, H., Isaksen, I., Jenkin, M., Kaiser, J., Kanakidou, M., Klimont, Z., Kulmala, M., Laj, P., Lawrence, M., Lee, J., Liousse, C., Maione, M., McFiggans, G., Metzger, A., Mieville, A., Moussiopoulos, N., Orlando, J., O'Dowd, C., Palmer, P., Parrish, D., Petzold, A., Platt, U., Pöschl, U., Prévôt, A., Reeves, C., Reimann, S., Rudich, Y., Sellegri, K., Steinbrecher, R., Simpson, D., ten Brink, H., Theloke, J., van der Werf, G., Vautard, R., Vestreng, V., Vlachokostas, C., and von Glasow, R.: Atmospheric composition change – global and regional air quality, Atmos. Environ., 43, 5268–5350, doi:10.1016/j.atmosenv.2009.08.021, 2009.

Parrish, D. D., Singh, H. B., Molina, L., and Madronich, S.: Air quality progress in North American megacities: a review, Atmos. Environ., 45, 7015–7025, doi:10.1016/j.atmosenv.2011.09.039, 2011.

Richter, A., Burrows, J. P., Nüss, H., Granier, C., and Niemeier, U.: Increase in tropospheric nitrogen dioxide over China observed from space, Nature, 437, 129–32, doi:10.1038/nature04092, 2005.

Russell, A. R., Valin, L. C., and Cohen, R. C.: Trends in OMI NO_2 observations over the United States: effects of emission control technology and the economic recession, Atmos. Chem. Phys., 12, 12197–12209, doi:10.5194/acp-12-12197-2012, 2012.

Santer, B., Wigley, T., Boyle, J., Gaffen, D., Hnilo, J., Nychka, D., Parker, D., and Taylor, K.: Statistical significance of trends and trend differences in layer-average atmospheric temperature time series, J. Geophys. Res., 105, 7337–7356, 2000.

Schaub, D., Brunner, D., Boersma, K. F., Keller, J., Folini, D., Buchmann, B., Berresheim, H., and Staehelin, J.: SCIAMACHY tropospheric NO_2 over Switzerland: estimates of NO_x lifetimes and impact of the complex Alpine topography on the retrieval, Atmos. Chem. Phys., 7, 5971–5987, doi:10.5194/acp-7-5971-2007, 2007.

Schneider, P. and van der A, R. J.: A global single-sensor analysis of 2002–2011 tropospheric nitrogen dioxide trends observed from space, J. Geophys. Res., 117, 1–17, doi:10.1029/2012JD017571, 2012.

Sitnov, S. a.: Analysis of satellite observations of the tropospheric NO2 content over the Moscow region , Izvestiya, Atmospheric and Oceanic Physics, 47, 166–185, doi:10.1134/S0001433811010129, http://link.springer.com/10.1134/S0001433811010129, 2011.

Tiao, G., Reinsel, G. C., Daming, X., Pedrick, J. H., Xiaodong, Z., Miller, A. J., DeLuisi, J. J., Mateer, C. L., and Wuebbles, D. J.: Effects of autocorrelation and temporal sampling schemes on estimates of trend and spatial correlation, J. Geophys. Res., 95, 20507–20517, 1990.

United Nations: World Urbanization Prospects The 2011 Revision – Highlights, Tech. rep., United Nations – Department of Economic and Social Affairs – Population Division, New York, NY, 2012a.

United Nations: World Urbanization Prospects: The 2011 Revision – CD-ROM Edition, available at: http://esa.un.org/unpd/wpp/index.htm (last access: 2 June 2014), 2012b.

van der A, R. J., Peters, D. H. M. U., Eskes, H., Boersma, K. F., Van Roozendael, M., De Smedt, I., and Kelder, H. M.: Detection of the trend and seasonal variation in tropospheric NO_2 over China, J. Geophys. Res., 111, 1–10, doi:10.1029/2005JD006594, 2006.

van der A, R. J., Eskes, H. J., Boersma, K. F., van Noije, T. P. C., Van Roozendael, M., De Smedt, I., Peters, D. H. M. U., and Meijer, E. W.: Trends, seasonal variability and dominant NO_x source derived from a ten year record of NO_2 measured from space, J. Geophys. Res., 113, 1–12, doi:10.1029/2007JD009021, 2008.

Vrekoussis, M., Richter, A., Hilboll, A., Burrows, J. P., Gerasopoulos, E., Lelieveld, J., Barrie, L., Zerefos, C., and Mihalopoulos, N.: Economic crisis detected from space: air quality observations over Athens/Greece, Geophys. Res. Lett., 40, 458–463, doi:10.1002/grl.50118, 2013.

Weatherhead, E., Reinsel, G., Tiao, G., Meng, X., Choi, D., Cheang, W., Keller, T., DeLuisi, J., Wuebbles, D., Kerr, J., and Others: Factors affecting the detection of trends: statistical considerations and applications to environmental data, J. Geophys. Res.-Atmos., 103, 17149–17161, 1998.

World Health Organization : Review of evidence on health aspects of air pollution – REVIHAAP Project , Tech. rep., Copenhagen, Denmark, 2013.

Zhou, Y., Brunner, D., Hueglin, C., Henne, S., and Staehelin, J.: Changes in OMI tropospheric NO2 columns over Europe from 2004 to 2009 and the influence of meteorological variability , Atmospheric Environment, 46, 482–495, doi:10.1016/j.atmosenv.2011.09.024, http://linkinghub.elsevier.com/retrieve/pii/S1352231011009654, 2012.

Zhu, T., Melamed, M. L., Parrish, D., Gauss, M., Gallardo Klenner, L., Lawrence, M., Konare, A., and Liousse, C.: Impacts of Megacities on Air Pollution and Climate, Tech. Rep. 205, WMO/IGAC, Geneva, Switzerland, 2012.

Table 1. Metadata of the selected megacities and other large urban agglomerations. A total of 66 sites were selected based on the criteria listed in Sect. 3.2. The given latitude and longitude values indicate the location at which the time series was extracted from the SCIAMACHY dataset. The data on estimated population was taken from United Nations (2012b).

City Name	Country	Lat. [° N]	Lon. [° E]	Pop. [mill.]
Algiers	Algeria	36.76	3.04	3.4
Athens	Greece	37.98	23.73	3.6
Atlanta	USA	33.76	−84.39	5.4
Baghdad	Iraq	33.32	44.40	6.4
Bangalore	India	12.97	77.60	9.5
Bangkok	Thailand	13.72	100.54	14.3
Beijing	China	39.91	116.37	16.9
Bogota	Colombia	4.65	−74.10	9.2
Boston	USA	42.37	−71.07	7.2
Buenos Aires	Argentina	−34.62	−58.46	14.5
Cairo	Egypt	30.04	31.24	16.0
Chengdu	China	30.66	104.06	6.4
Chicago	USA	41.88	−87.67	9.8
Chongqing	China	29.56	106.55	6.4
Damascus	Syria	33.51	36.30	3.5
Delhi	India	28.63	77.22	23.7
Dhaka	Bangladesh	23.74	90.40	16.0
Guangzhou	China	23.13	113.24	26.4
Ho Chi Minh City	Vietnam	10.78	106.66	8.1
Hong Kong	China	22.32	114.18	7.2
Houston	USA	29.76	−95.37	5.9
Hyderabad	India	17.39	78.48	8.5
Istanbul	Turkey	41.01	28.97	13.6
Jakarta	Indonesia	−6.22	106.85	26.0
Jeddah	Saudi Arabia	21.53	39.20	3.9
Johannesburg	South Africa	−26.20	28.04	8.5

Table 1. Continued.

City Name	Country	Lat. [° N]	Lon. [° E]	Pop. [mill.]
Kabul	Afghanistan	34.53	69.17	3.5
Karachi	Pakistan	24.88	67.04	22.3
Khartoum	Sudan	15.55	32.53	5.2
Kinshasa	Congo	−4.34	15.31	9.8
Kolkata	India	22.57	88.36	15.9
Lagos	Nigeria	6.51	3.35	13.0
Lahore	Pakistan	31.51	74.34	9.4
Lima	Peru	−12.05	−77.04	9.6
London	Great Britain	51.51	−0.11	13.3
Los Angeles	USA	33.92	−118.08	17.1
Madras	India	13.07	80.22	9.5
Manila	Philippines	14.61	121.02	21.9
Melbourne	Australia	−37.80	145.05	4.2
Mexico City	Mexico	19.42	−99.13	23.6
Moscow	Russia	55.75	37.62	16.3
Mumbai	India	19.08	72.88	21.2
Nagoya	Japan	35.19	136.85	8.5
Nairobi	Kenya	−1.29	36.83	4.7
New York	USA	40.76	−73.97	21.6
Osaka	Japan	34.65	135.51	16.8
Paris	France	48.86	2.35	10.6
Philadelphia	USA	39.96	−75.16	7.3
Po Valley	Italy	45.47	9.19	24.3
Rhein-Ruhr	Germany	51.49	7.08	4.6
Rio de Janeiro	Brazil	−22.85	−43.32	12.8
Riyadh	Saudi Arabia	24.69	46.73	6.1

Table 1. Continued.

City Name	Country	Lat. [° N]	Lon. [° E]	Pop. [mill.]
San Francisco	USA	37.75	−122.43	7.2
Santiago	Chile	−33.46	−70.64	6.3
Sao Paulo	Brazil	−23.55	−46.64	21.4
Seoul	Korea (South)	37.54	126.97	25.6
Shanghai	China	31.23	121.48	26.0
Shenyang	China	41.81	123.43	7.3
Shenzhen	China	22.58	114.05	10.1
Sydney	Australia	−33.91	151.06	4.7
Taipei	Taiwan	25.04	121.51	9.0
Tehran	Iran	35.70	51.41	13.8
Tianjin	China	39.14	117.20	10.1
Tokyo	Japan	35.70	139.76	34.7
Washington	USA	38.90	−77.02	8.1
Wuhan	China	30.56	114.32	9.3

Table 2. Extreme values among the studied large urban agglomerations, both in terms of absolute and relative trends. All of the listed trends are statistically significant at the $p < 0.05$ level.

	Absolute Trends	Relative Trends
Largest positive	Tianjin, China $2.83(\pm 0.48) \times 10^{15}$ molecules $\mathrm{cm^{-2}\,yr^{-1}}$	Kabul, Afghanistan $14.3(\pm 2.2)\,\%\,\mathrm{yr^{-1}}$
Largest negative	Los Angeles, USA $-1.66(\pm 0.31) \times 10^{15}$ molecules $\mathrm{cm^{-2}\,yr^{-1}}$	Boston, USA $-9.0(\pm 3.0)\,\%\,\mathrm{yr^{-1}}$

Table 3. Trend analysis results for all studied large urban agglomerations. The absolute trends and their uncertainty are given in units of $\times 10^{15}$ molecules cm^{-2} yr^{-1} and the relative trends and their uncertainty are given in % yr^{-1}. The trends shown here were computed using time series extracted from a single grid cell located over the center of each agglomeration. The relative trends were computed with respect to the long term mean of the time series over a given grid cell. Trends that were found to be statistically significant at the $p < 0.05$ level are marked in bold. N indicates the total number of months in the time series with valid data.

City	N	Absolute Trend	Relative Trend
Algiers	115	0.096 ± 0.066	2.4 ± 1.7
Athens	114	$\mathbf{-0.213 \pm 0.081}$	$\mathbf{-3.6 \pm 1.4}$
Atlanta	108	$\mathbf{-0.449 \pm 0.111}$	$\mathbf{-5.4 \pm 1.3}$
Baghdad	115	$\mathbf{0.600 \pm 0.085}$	$\mathbf{8.5 \pm 1.2}$
Bangalore	87	$\mathbf{0.188 \pm 0.058}$	$\mathbf{6.1 \pm 1.9}$
Bangkok	116	0.203 ± 0.163	1.9 ± 1.6
Beijing	110	0.152 ± 0.552	0.4 ± 1.3
Bogota	38	$\mathbf{-0.250 \pm 0.091}$	$\mathbf{-3.4 \pm 1.2}$
Boston	108	$\mathbf{-0.828 \pm 0.281}$	$\mathbf{-9.0 \pm 3.0}$
Buenos Aires	113	$\mathbf{0.249 \pm 0.107}$	$\mathbf{3.1 \pm 1.3}$
Cairo	116	$\mathbf{0.414 \pm 0.067}$	$\mathbf{5.0 \pm 0.8}$
Chengdu	73	$\mathbf{1.248 \pm 0.221}$	$\mathbf{8.0 \pm 1.4}$
Chicago	113	$\mathbf{-0.684 \pm 0.191}$	$\mathbf{-5.1 \pm 1.4}$
Chongqing	67	$\mathbf{1.529 \pm 0.290}$	$\mathbf{10.2 \pm 1.9}$
Damascus	115	$\mathbf{0.185 \pm 0.089}$	$\mathbf{3.1 \pm 1.5}$
Delhi	112	0.125 ± 0.110	1.4 ± 1.2
Dhaka	107	$\mathbf{0.525 \pm 0.063}$	$\mathbf{10.3 \pm 1.2}$
Guangzhou	91	-0.252 ± 0.417	-0.8 ± 1.4
Ho Chi Minh City	108	0.049 ± 0.044	1.4 ± 1.3
Hong Kong	105	-0.424 ± 0.282	-2.5 ± 1.7
Houston	107	$\mathbf{-0.540 \pm 0.157}$	$\mathbf{-5.4 \pm 1.6}$
Hyderabad	109	$\mathbf{0.142 \pm 0.056}$	$\mathbf{4.7 \pm 1.9}$
Istanbul	108	-0.047 ± 0.230	-0.4 ± 1.9

Table 3. Continued.

City	N	Absolute Trend	Relative Trend
Jakarta	108	-0.241 ± 0.150	-2.1 ± 1.3
Jeddah	115	0.102 ± 0.086	1.6 ± 1.3
Johannesburg	111	$\mathbf{-0.488 \pm 0.193}$	$\mathbf{-3.1 \pm 1.2}$
Kabul	110	$\mathbf{0.299 \pm 0.046}$	$\mathbf{14.3 \pm 2.2}$
Karachi	113	$\mathbf{0.194 \pm 0.064}$	$\mathbf{4.0 \pm 1.3}$
Khartoum	116	0.018 ± 0.035	1.5 ± 2.9
Kinshasa	80	0.036 ± 0.035	1.5 ± 1.4
Kolkata	109	$\mathbf{0.114 \pm 0.063}$	$\mathbf{2.6 \pm 1.4}$
Lagos	83	$\mathbf{0.265 \pm 0.050}$	$\mathbf{7.8 \pm 1.5}$
Lahore	113	$\mathbf{0.334 \pm 0.087}$	$\mathbf{6.0 \pm 1.6}$
Lima	75	$\mathbf{0.363 \pm 0.108}$	$\mathbf{6.9 \pm 2.0}$
London	107	-0.255 ± 0.205	-1.7 ± 1.4
Los Angeles	113	$\mathbf{-1.656 \pm 0.308}$	$\mathbf{-5.8 \pm 1.1}$
Madras	106	$\mathbf{0.151 \pm 0.058}$	$\mathbf{3.9 \pm 1.5}$
Manila	102	$\mathbf{-0.363 \pm 0.074}$	$\mathbf{-6.0 \pm 1.2}$
Melbourne	111	-0.103 ± 0.082	-1.6 ± 1.3
Mexico City	104	-0.354 ± 0.276	-1.3 ± 1.0
Moscow	95	-0.185 ± 0.273	-1.2 ± 1.8
Mumbai	103	0.037 ± 0.077	0.6 ± 1.2
Nagoya	101	-0.400 ± 0.244	-2.3 ± 1.4
Nairobi	88	$\mathbf{0.172 \pm 0.040}$	$\mathbf{13.1 \pm 3.0}$
New York	113	$\mathbf{-0.950 \pm 0.310}$	$\mathbf{-4.3 \pm 1.4}$
Osaka	110	$\mathbf{-0.445 \pm 0.231}$	$\mathbf{-2.7 \pm 1.4}$
Paris	108	$\mathbf{-0.471 \pm 0.171}$	$\mathbf{-3.3 \pm 1.2}$
Philadelphia	109	$\mathbf{-0.917 \pm 0.205}$	$\mathbf{-5.9 \pm 1.3}$
Po Valley	112	$\mathbf{-0.621 \pm 0.214}$	$\mathbf{-3.4 \pm 1.2}$
Rhein-Ruhr	104	$\mathbf{-0.452 \pm 0.219}$	$\mathbf{-2.8 \pm 1.4}$
Rio de Janeiro	102	-0.073 ± 0.090	-0.9 ± 1.1
Riyadh	115	$\mathbf{0.270 \pm 0.133}$	$\mathbf{2.1 \pm 1.1}$

Table 3. Continued.

City	N	Absolute Trend	Relative Trend
San Francisco	113	$\mathbf{-0.442 \pm 0.124}$	$\mathbf{-5.0 \pm 1.4}$
Santiago	115	$\mathbf{0.270 \pm 0.106}$	$\mathbf{2.8 \pm 1.1}$
Sao Paulo	104	-0.006 ± 0.161	0.0 ± 1.0
Seoul	105	-0.576 ± 0.517	-1.9 ± 1.7
Shanghai	106	$\mathbf{1.306 \pm 0.347}$	$\mathbf{4.2 \pm 1.1}$
Shenyang	106	$\mathbf{1.705 \pm 0.278}$	$\mathbf{9.4 \pm 1.5}$
Shenzhen	101	$\mathbf{-0.842 \pm 0.351}$	$\mathbf{-3.8 \pm 1.6}$
Sydney	111	$\mathbf{-0.239 \pm 0.116}$	$\mathbf{-2.9 \pm 1.4}$
Taipei	96	0.040 ± 0.209	0.4 ± 2.1
Tehran	115	$\mathbf{0.634 \pm 0.216}$	$\mathbf{3.2 \pm 1.1}$
Tianjin	110	$\mathbf{2.831 \pm 0.480}$	$\mathbf{7.7 \pm 1.3}$
Tokyo	108	$\mathbf{-1.282 \pm 0.306}$	$\mathbf{-4.9 \pm 1.2}$
Washington	112	$\mathbf{-0.740 \pm 0.184}$	$\mathbf{-6.3 \pm 1.6}$
Wuhan	107	$\mathbf{1.063 \pm 0.188}$	$\mathbf{6.4 \pm 1.1}$

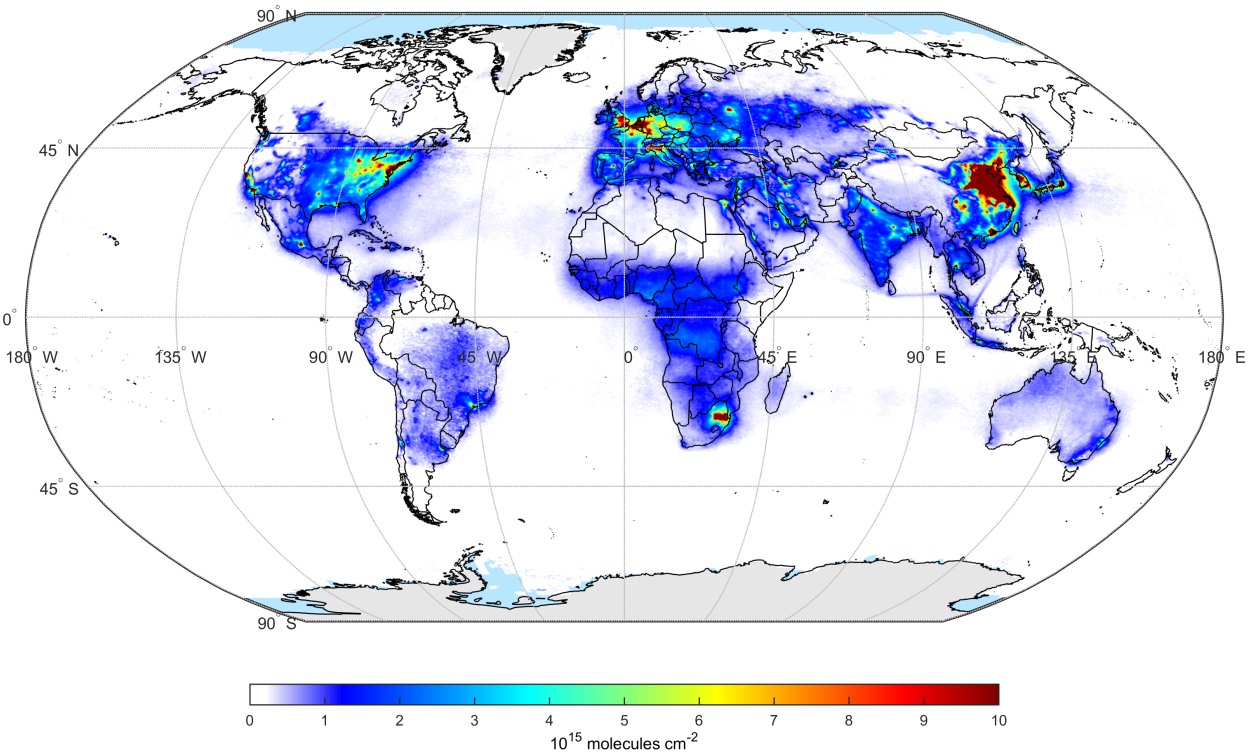

Figure 1. Global map of long-term average tropospheric NO_2 column derived from SCIAMACHY data (given in units of $\times 10^{15}$ molecules cm^{-2}). The average was computed over the entire usable time series of SCIAMACHY data ranging from August 2002 to March 2012. The faint linear feature in the North Atlantic is not a real signal but an artefact of the retrieval process. It does not affect the analysis of trends in urban agglomerations presented here.

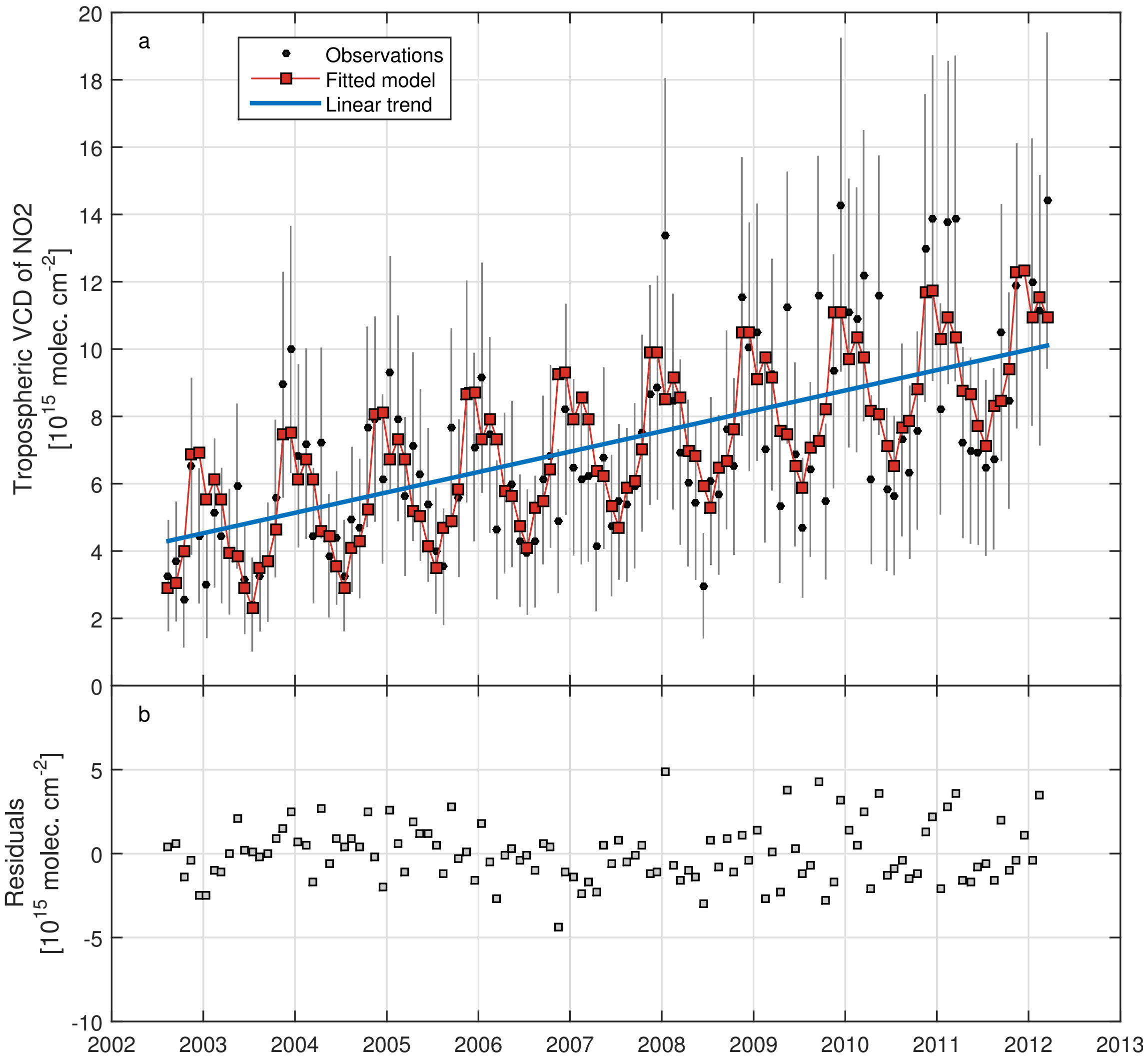

a
Observations
Fitted model
Linear trend
Tropospheric VCD of NO2
[10^{15} molec. cm^{-2}]
b
Residuals
[10^{15} molec. cm^{-2}]
2002
2003
2004
2005
2006
2007
2008
2009
2010
2011
2012
2013

Figure 2. Global map Example of relative 2002–2012 a SCIAMACHY-derived time series of monthly mean tropospheric NO_2 trends over all studied urban agglomerations. The relative trends are column (given with respect to the long-term average concentration computed over the entire time series at each grid cell individually. The names in units of all $\times 10^{15}$ molecules cm^{-2}) including estimated uncertainty for the studies urban agglomerations as well as the exact absolute city of Baghdad, Iraq and relative the fitted statistical model including linear trend values for each site can be found (top) and the corresponding residuals of the fitted model (bottom) (given in Table 3 units of $\times 10^{15}$ molecules cm^{-2}) .

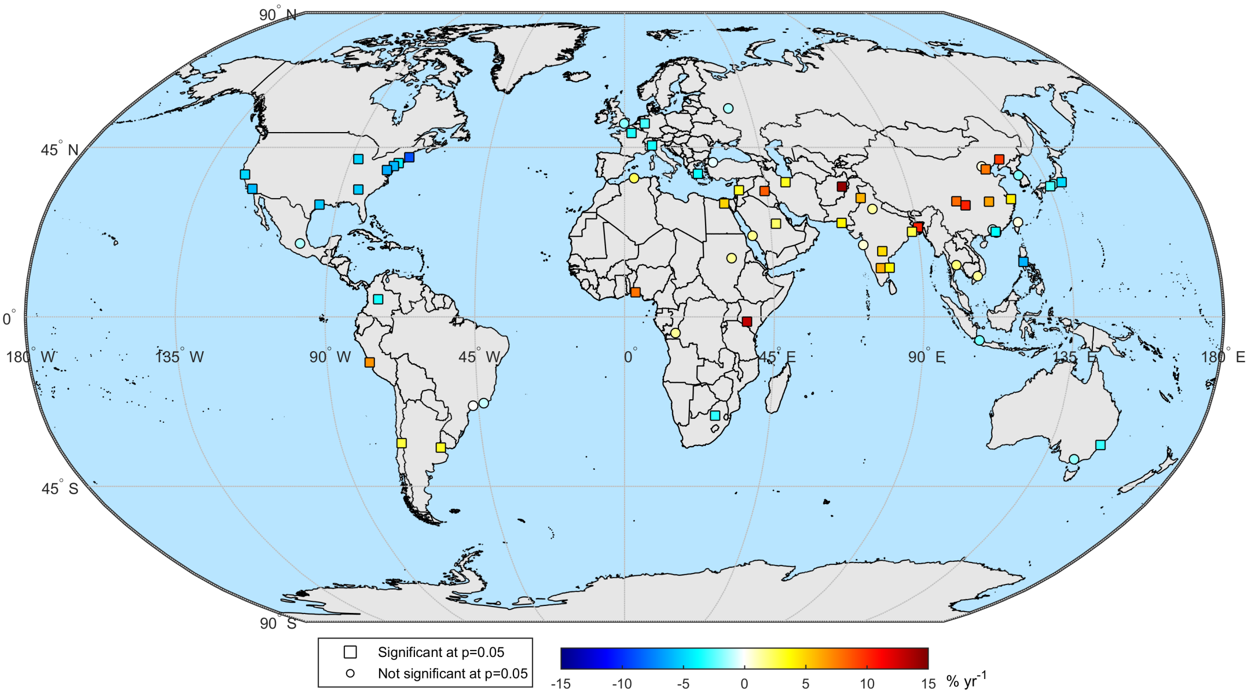

Figure 3. Global map of relative 2002–2012 tropospheric NO_2 trends over all studied urban agglomerations. The relative trends in units of % yr^{-1} are given with respect to the long-term average concentration computed over the entire time series at each grid cell individually. The names of all the studied urban agglomerations as well as the exact absolute and relative trend values for each site can be found in Table 3.

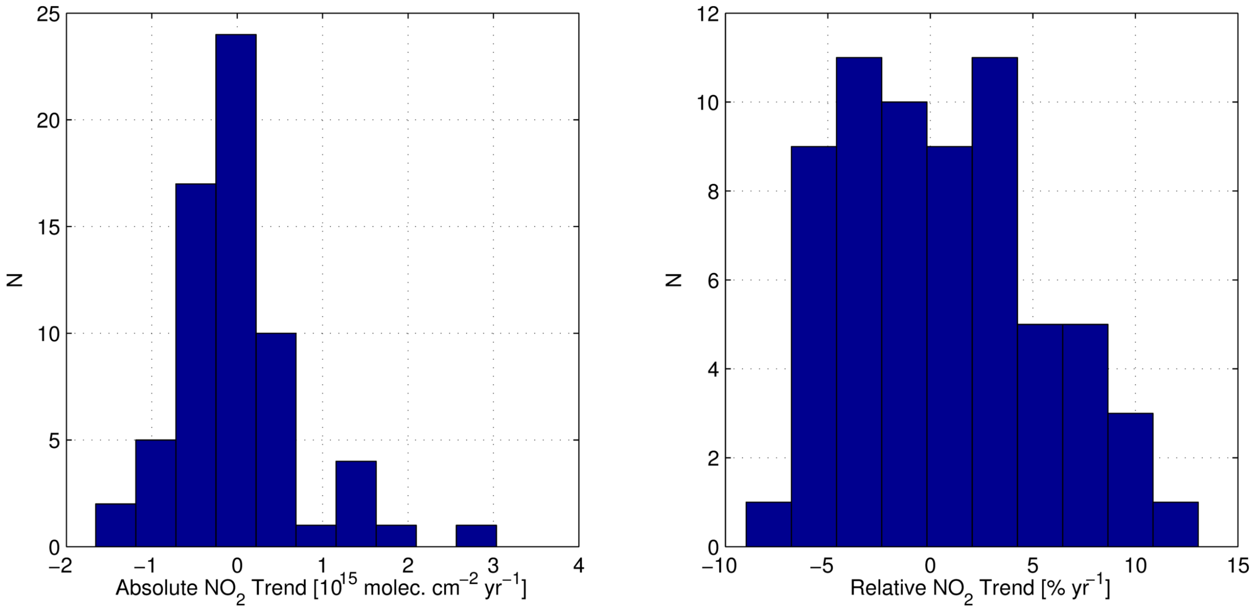

Figure 4. Histograms of absolute (left panel) and relative (right panel) tropospheric NO_2 trend trends over large urban agglomerations worldwide. The relative trends were computed with respect to the long-term average concentration computed over the entire time series at each grid cell individually.

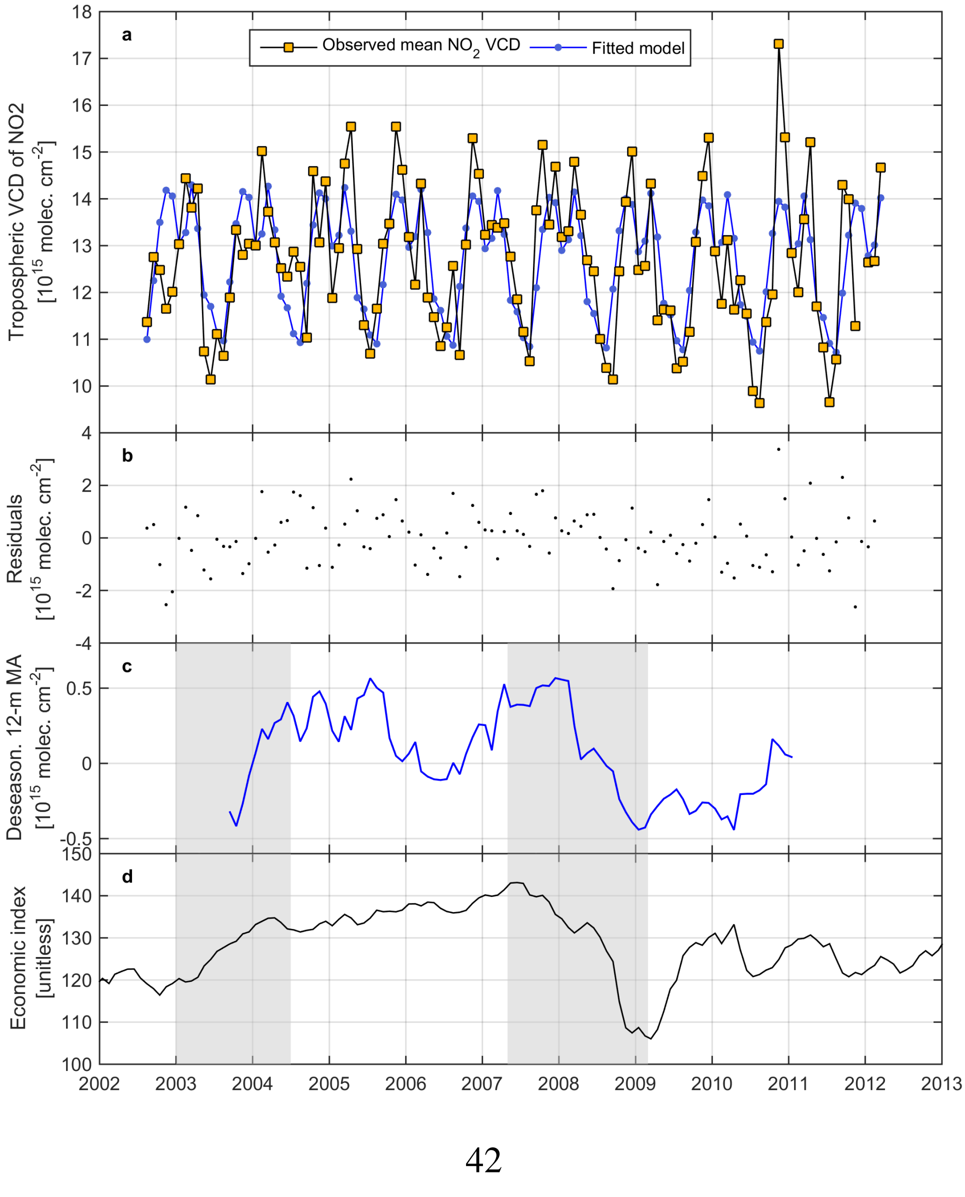

a
Observed mean NO2 VCD
Fitted model
Tropospheric VCD of NO2
[10^15 molec. cm^-2]
b
Residuals
[10^15 molec. cm^-2]
c
Deseason. 12-m MA
[10^15 molec. cm^-2]
d
Economic index
[unitless]
2002
2003
2004
2005
2006
2007
2008
2009
2010
2011
2012
2013

Figure 5. Average time series of SCIAMACHY-derived tropospheric NO_2 column computed over all study sites including a fitted trend model (top a)and , the model residuals (b), the 12-month moving average of the deseasonalized time series (bottom c), and the ECRI Weekly Economic Index . In order Gray boxes in the two lowermost panels mark periods where the overall NO_2 levels in the studied urban agglomerations appear to obtain a representative estimate, a monthly mean was only computed when at least a minimum be indicative of 40 sites provided valid data for that particular month overall economic activity .

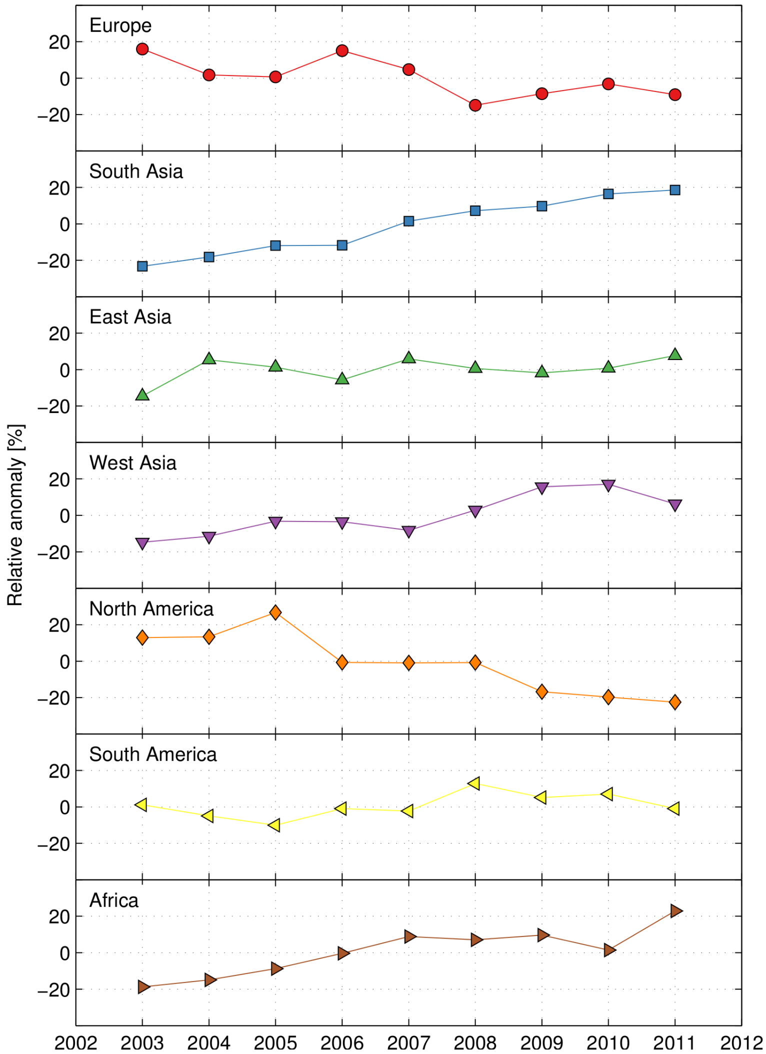

Figure 6. Interannual variability of NO_2 over large urban agglomerations, averaged by region. To facilitate an easier comparison between regions, the plot shows the average of the relative anomaly (given in % yr^{-1}) of each sites' time series within a given region. The anomalies were computed relative to the long-term mean absolute NO_2 concentration at each site.

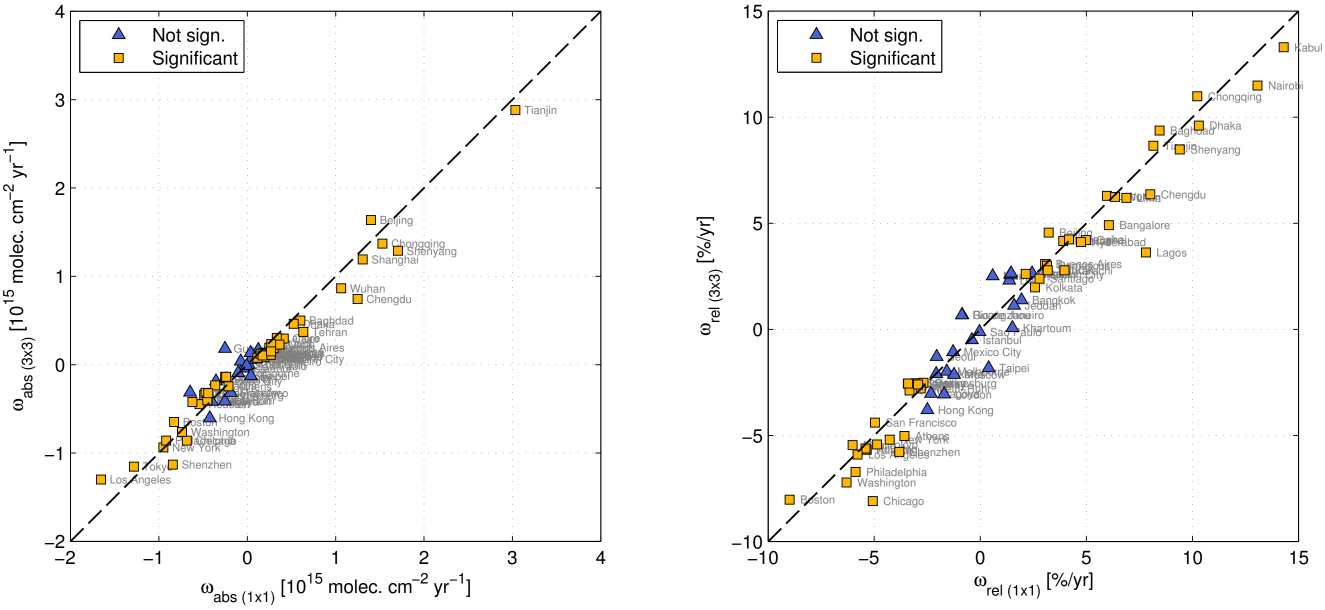

Figure 7. Comparison of absolute (left panel) and relative (right panel) trends calculated using time series extracted from a single SCIAMACHY grid cell ($\omega_{\mathrm{abs}(1\times1)}$ and $\omega_{\mathrm{rel}(1\times1)}$) and as the average of an array of 3×3 SCIAMACHY grid cells ($\omega_{\mathrm{abs}(3\times3)}$ and $\omega_{\mathrm{rel}(3\times3)}$). The markers are further distinguished into trends that are statistically significant at the $p < 0.05$ level (blue triangles) and those that are not (yellow squares) .

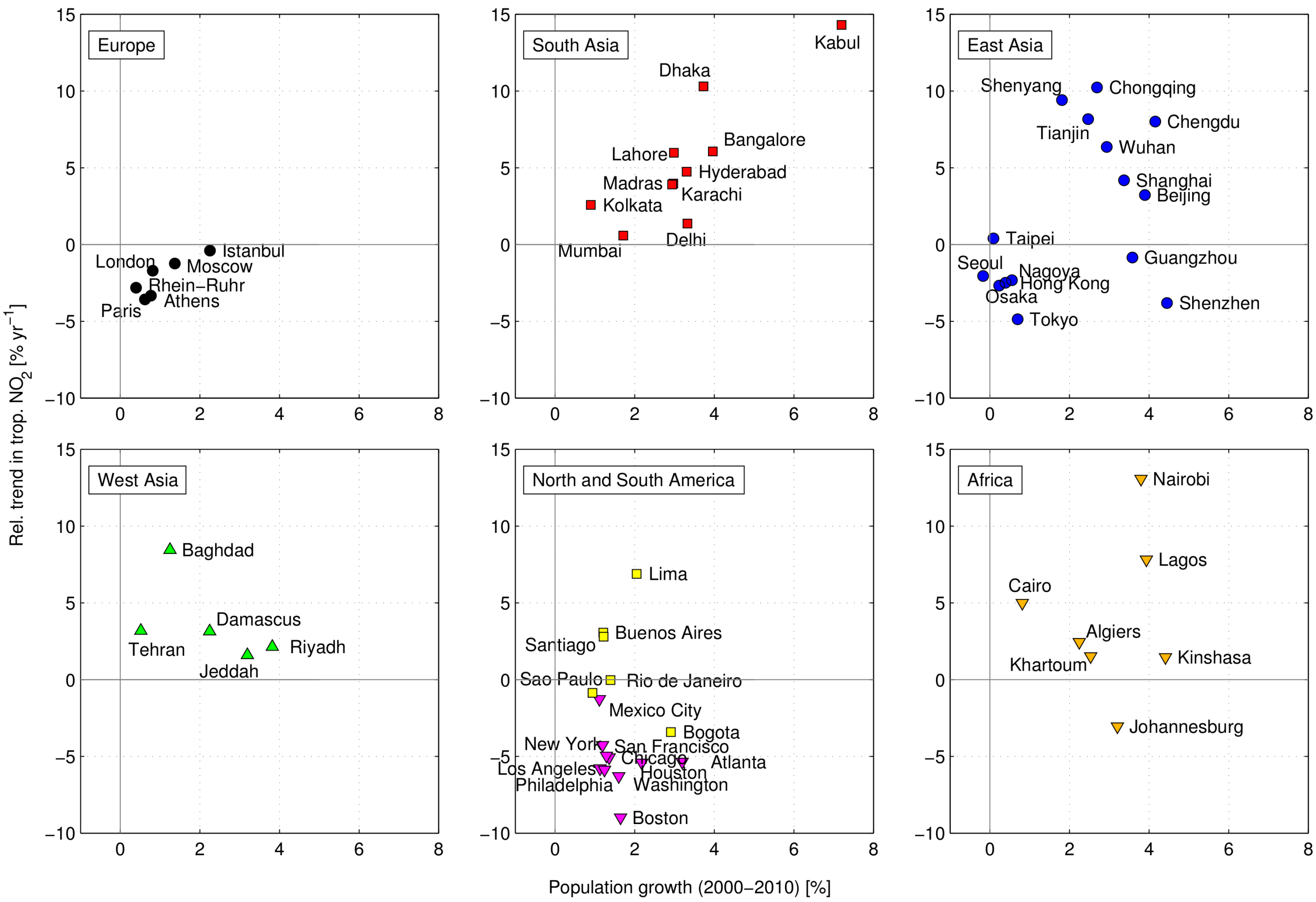

Figure 8. Relationship between population growth for the period 2000 and 2010 and SCIAMACHY-derived trends in tropospheric NO_2 for 2002 to 2012, by region. North and Souther America was combined into a single panel, where data points in North America are shown as pink triangles and data points in South America are shown as yellow squares .